S. pombe DNA translocases Rrp1 and Rrp2 have distinct roles at centromeres and telomeres that ensure genome stability

Article (Accepted Version)

S. pombe DNA translocases Rrp1 and Rrp2 have distinct roles at centromeres and telomeres that ensure genome stability

Anna Barg-Wojas[1], Jakub Muraszko[1#], Karol Kramarz[2#], Kamila Schirmeisen[1,4], Gabriela Baranowska[1], Antony M. Carr[3], Dorota Dziadkowiec[1,*]

[1] Faculty of Biotechnology, University of Wrocław, Poland

[2] Institut Curie, Centre National de la Recherche Scientifique, Orsay, France

[3] Genome Damage and Stability Centre, School of Life Sciences, University of Sussex, BN1 9RQ, United Kingdom

[4] present address: Institut Curie, Centre National de la Recherche Scientifique, Orsay, France

[#] these authors contributed equally to this work

* corresponding author: dorota.dziadkowiec@uwr.edu.pl

Key words: nucleosome dynamics; DNA translocase; centromere and telomere structure

SUMMARY STATEMENT

Schizosaccharomyces pombe DNA translocases Rrp1 and Rrp2 modulate nucleosome dynamics to maintain centromere and telomere function and dysregulation of their activity leads to genome instability.

ABSTRACT

The regulation of telomere and centromere structure and function is essential for maintaining genome integrity. *Schizosaccharomyces pombe* Rrp1 and Rrp2 are orthologues of *Saccharomyces cerevisiae* Uls1, a SWI2/SNF2 DNA translocase and SUMO-Targeted Ubiquitin Ligase. Here we show that Rrp1 or Rrp2 overproduction leads to chromosome instability and growth defects, a reduction of global histone levels and mislocalisation of centromere-specific histone Cnp1. These phenotypes depend on putative DNA translocase activities of Rrp1 and Rrp2, suggesting that Rrp1 and Rrp2 may be involved in modulating nucleosome dynamics. Furthermore, we confirm that Rrp2, but not Rrp1, acts at telomeres, reflecting a previously described interaction between Rrp2 and Top2. In conclusion, we identify roles for Rrp1 and Rrp2 in maintaining centromere function by modulating histone dynamics, contributing to the preservation of genome stability during vegetative cell growth.

JCS Advance Online Article. Posted on 13 January 2020

INTRODUCTION

We previously identified a role for Rrp1 and Rrp2 in Rad51-dependent homologous recombination (HR). HR is a highly conserved pathway that functions during DNA replication, participates in the repair of double strand breaks (DSBs) during interphase and is essential for meiosis. *Schizosaccharomyces pombe* Rad51 is aided by two mediator complexes that act in parallel to promote Rad51-dependent strand exchange: Rad55-Rad57 and Sfr1-Swi5 (Akamatsu et al., 2007), both of which are conserved in humans (Yuan and Chen, 2011). Rrp1 and Rrp2 act in a mutually dependent manner in the Swi5/Sfr1-mediated sub-pathway of HR (Dziadkowiec et al., 2009) to negatively regulate one or more sub-pathways of Rad51-mediated recombination (Dziadkowiec et al., 2013). Both Rrp1 and Rrp2 are orthologues of *S. cerevisiae* Uls1, a SWI2/SNF2 DNA translocase and SUMO-Targeted Ubiquitin Ligase (STUbL).

Telomeres and centromeres are potentially difficult to replicate regions due to the presence of repetitive sequences that can form secondary structures. These repetitive sequences are often unstable and constitute the hotspots of replication fork arrest and recombination. HR proteins act at arrested replication forks: Rad51 binding promotes the stability of the fork itself (Mizuno et al., 2013; Schlacher et al., 2011) whereas, when the fork is inactivated, the strand exchange activity of Rad51 promotes the reconstitution of replication (Lambert et al., 2005; McGlynn and Lloyd, 2002). Indeed, *S. pombe* Rad51 localises to centromeres (Nakamura et al., 2008) and loss of HR results in multiple changes to centromere function including repeat rearrangements, impaired transcriptional repression and elevated levels of chromosome loss (Onaka et al., 2016).

The *S. pombe* telomere binding protein Taz1 (and, in mammals, its orthologue TRF1) attenuates the tendency of telomere repeats to block replication (Miller et al., 2005; Sfeir et al., 2009). In *taz1*Δ mutants, replication forks arrested at telomeres are incorrectly processed leading to telomeric entanglements that cannot be resolved at temperatures below 20°C. The consequence of this is the formation of chromosome bridges, chromosome mis-segregation and reduced cell viability (Miller and Cooper, 2003). Topoisomerase II (Top2) mutants characterized by slower catalytic turnover (such as *top2-191*) are able to supress *taz1*Δ telomeric entanglement phenotypes (Germe et al., 2009). It was recently reported that Rrp2 acts independently of Rrp1 to protect cells from Top2-induced DNA damage and that its absence is toxic in the *top2-191* mutant (Wei et al., 2017). This suggested a role for Rrp2 in telomere replication. This function is shared with its *S. cerevisiae* orthologue, Uls1, which has been shown to inhibit nonhomologous end joining at telomeres (Lescasse et al., 2013) and to protect the cells against Top2 poisons in a manner dependent on its ATPase activity and SUMO-binding (Swanston et al., 2019; Wei et al., 2017).

Accumulating data clearly demonstrate that DNA metabolic processes at vulnerable regions of the genome are finely tuned to ensure genome stability. The activities involved are often distinguishable from those invoked in response to accute global DNA damage or replication stress. Consistent with this, Rrp2 has been shown to activate a specific meiotic recombination hotspot without affecting basal recombination levels (Storey et al., 2018) and, in *S. cerevisiae*, the relocation of DSBs flanked by repeat sequences (such as those found in telomeres) to nuclear pores depends on Uls1, but not on the general stress response STUbL, Slx5 (Marcomini et al., 2018). The opposite is true for DSB formed throughout the genome (Horigome et al., 2016).

The consequences of deleting genes encoding proteins that modulate DNA metabolic processes to accommodate specific genomic regions can often go undetected in experimental systems because the responses characteristic of acute DNA damage can substitute at the expense of modest defects in genome stability. However, dysregulation of these gene's activity through their over-expression can perturb the system more dramatically, generating abnormal replication and/or repair intermediates. This can lead to more extensive genomic instability and consequent viability loss. One such example in humans is *RECQ5*. Mutations in this gene are not directly associated with predisposition to cancer or genetic disease, but its amplification and increased expression is found in many tumours and has been shown to redirect repair to different pathways, leading to genomic instability (Olson et al., 2018).

The deletion of Rrp1 or Rrp2 leads to subtle phenotypes, often only uncovered by co-deletion of additional DNA repair proteins (Dziadkowiec et al., 2009). We thus exploited over-expression analysis to identify novel biological functions for these proteins. We report that Rrp1 and Rrp2 are involved in the maintenance of centromere function, but that, unlike their role in HR, these phenotypes are not mutually dependent and the role of Rrp1 is more pronounced than that of Rrp2. We find that Rrp1 and Rrp2 over-expression results in a decrease in the level of histone proteins in the cell and the spreading of Cnp1 (CENP-A; the specialised H3 ortholog required for centromere function) away from the central core of the centromere. Structure-function analysis of *rrp1* and *rrp2* alleles correlated these phenotypes to their putative translocase activities, suggesting that Rrp1 and Rrp2 are histone translocases that modulate histone levels at specific chromosomal regions and in response to global genotoxic stress. We also confirm that Rrp2 has an Rrp1-independent function at telomeres (Wei et al. 2017), validating our approach of overexpression analysis.

RESULTS

Rrp1 and Rrp2 may have a role in centromere function

Rrp1 and Rrp2 are involved in the replication stress response in a Swi5-Sfr1 dependent branch of HR (Dziadkowiec et al., 2009; Dziadkowiec et al., 2013). HR factors, such as Rad51 and Rad54, are required for centromere stability and cells devoid of these proteins are sensitive to the microtubule-destabilizing agent thiabendazole (TBZ) (Onaka et al., 2016). We similarly found that a *rad57*Δ mutant is sensitive to TBZ, but that *swi5*Δ, *sfr1*Δ, *rrp1*Δ and *rrp2*Δ mutants were not. Consistent with previous observations that the DNA damage phenotypes of *rrp1*Δ or *rrp2*Δ are only evident upon deletion of *rad57*$^{+}$, a small increase in TBZ sensitivity was observed in *rad57*Δ*rrp1*Δ and *rad57*Δ*rrp2*Δ strains when compared to *rad57*Δ (Fig. S1A). This implies that Rrp1 and Rrp2 may have a role in centromere maintenance. Previous work (Li et al., 2013) has shown that replication fork stability is required, together with heterochromatin, to ensure centromere integrity. We thus reasoned that, in mutants sensitive to TBZ due to destabilization of heterochromatin at centromeres (Allshire et al., 1995; Ekwall et al., 1996), the requirement for HR proteins for replication fork stability would be more pronounced. Unexpectedly, we observed that *rrp1*+ or *rrp2*+ deletion slightly decreased TBZ sensitivity in *swi6*Δ background, and that in the *clr4*Δ mutant background deletion of *rrp1*+, but not of *rrp2*+, lead to the rescue of the growth defect (Fig. S1B). This suggests that Rrp1 (and likely Rrp2) contribute to centromere maintenance and, when heterochromatin structure is disrupted, their activity is deleterious.

Increase in Rrp1 and Rrp2 copy number results in chromosome instability and growth defect

In this context we reasoned that Rrp1 and Rrp2 overproduction would emphasise centromere-associated phenotypes in wild type cells and that this may be influenced by the deletion of *swi6*+ or *clr4*+. We thus examined the effect of *rrp1*+ or *rrp2*+ over-expression from the medium strength *nmt* promoter (*nmt41* and *42*). Indeed, over-expression caused viability loss and moderate TBZ sensitivity in otherwise wild type cells grown under unperturbed conditions (Fig. 1A). Moreover, the growth defect induced by either *rrp1*+ (Fig. S1C) or *rrp2*+ (Fig. S1D) over-expression in the *swi6*Δ mutant was exacerbated when compared to that seen in wild type cells and their over-expression strongly sensitized *swi6*Δ cells to TBZ. Furthermore, the viability loss caused by *rrp1*+ and *rrp2*+ over-expression in the *clr4*Δ mutant was greater than in WT or *swi6*Δ cells (Fig. S1C,D).

Microscopic examination of DAPI stained WT cells revealed that prolonged over-expression of *rrp1*+, and even more so of *rrp2*+, caused mitotic aberrations, including chromosome non-disjunction and "cut" nuclei (Fig. 1B). We observed in these cells the

appearance of exceptionally bright Rad11 (RPA) foci (Fig. 1C), which may result from excessive accumulation of ssDNA, as has been reported before (Mejia-Ramirez et al., 2015) in cells where replication was perturbed in the absence of γH2AX. Additionally, approximately 30% of anaphase cells over-expressing *rrp1*+ or *rrp2*+ accumulated fragmented DNA and bridges coated with Rad11 (Fig. 1C, marked with arrows), some of them resembling lagging chromosomes. This implies that chromosome segregation defects occur in these cells.

Problems associated with chromosome segregation result in chromosome instability (Murray et al., 1994). We used a strain with a nonessential Ch^{16} minichromosome carrying the *ade6-216* allele *trans*-complementing the endogenous *ade6-210* allele of the host cell to measure chromosome loss induced by *rrp1*+ and *rrp2*+ over-expression. In this assay cells that lose the minichromosome form red colonies when grown on medium with a limiting concentration of adenine. We show that *rrp1*+ or *rrp2*+ over-expression increases minichromosome loss 5-fold (Fig. 1D).

When considered together, these data suggest that dysregulation of Rrp1 or Rrp2 interferes with centromere function resulting in chromosome segregation defects and genetic instability.

Rrp1 and Rrp2 potentially influence centromere structure by modulation of histone levels

Misincorporation of *S. cerevisiae* CENP-A has been shown to result in chromosome instability in *S. cerevisiae* (Hildebrand and Biggins, 2016). In *S. pombe*, Cnp1 (CENP-A) misincorporation leads to defective kinetochore function and chromosome mis-segregation (Castillo et al., 2007). We thus performed ChIP of endogenously CFP-tagged Cnp1 and observed that either *rrp1*+ or *rrp2*+ over-expression lead to an increased Cnp1 enrichment at the core region of centromere (Fig. 2A). We also observed Cnp1 spreading to neighbouring *dg* regions (Fig. 2B), directly demonstrating that centromere structure is perturbed by *rrp1*+ and *rrp2*+ over-expression. It has been shown using fluorescence microscopy that upon Cnp1-GFP over-expression from intermediate strength promotor, Cnp1 foci appear somewhat stretched and assemble preferentially near heterochromatic regions (Gonzalez et al., 2014). The signal for Cnp1-CFP expressed from its endogenous promotor is very weak, but we were nevertheless able to detect upon *rrp1*+ and *rrp2*+ over-expression a significant increase in the incidence of aberrant Cnp1 foci (Fig. 2C), indicating that Cnp1 is indeed mislocalised in these cells.

While cells over-expressing *rrp1*+ or *rrp2*+ did not show any statistically significant increase in Cnp1 levels (Fig. 2D,E), we noticed that the total levels of histone H3 were reduced (Fig. 2D,F). Thus, the ratio of Cnp1 to H3 increased (Fig. 2G). This was especially evident in Rrp1 over-producing cells, consistent with the stronger effect on TBZ sensitivity

and silencing. It has been reported that endogenous Cnp1 (CENP-A) may be redistributed away from the centromeric central domain when classical H3 nucleosome assembly is perturbed (Choi et al., 2012). Thus, the defects in chromosome segregation observed upon *rrp1*+ and, to a lesser extent, *rrp2*+ over-expression, correlate with H3 nucleosome depletion and Cnp1 mislocalisation.

In *S. pombe*, loss of transcriptional silencing at the centromere is an indicator of the disruption of centromere structure (Allshire et al., 1995). Similarly, the genomic instability due to CENP-A misincorporation in *S. cerevisiae* was accompanied by transcriptional defects (Hildebrand and Biggins, 2016). We thus examined the effect of Rrp1 and Rrp2 on silencing by assaying functional expression of an *ade6*+ gene that is inserted into the *dg* region of centromere 1 (*dg-ade6*+: Fig. 3A). Similarly to TBZ sensitivity phenotypes, we do not see any effect of *rrp1*+ or *rrp2*+ deletion on the silencing of *dg-ade6*+ in *swi6*+ or *swi6*Δ backgrounds, as determined by the lack of growth on plates devoid of adenine (Fig. S2A). However, *rrp1*+ or *rrp2*+ over-expression moderately increased transcriptional repression of the *dg-ade6*+ gene in a *swi6*+ background (Fig. S2B). In a *swi6*Δ background, *rrp1*+ over-expression partially reversed the transcriptional de-repression of *dg-ade6*+ (Fig. 3B). The strong viability loss conferred by *rrp2*+ over-expression made it more difficult to assess its role in silencing. We can, however, observe in these cells an increase in the repression of *dg-ade6*+ (Fig. 3B), albeit less significant than that seen for *rrp1*+. The increase of transcriptional repression that we observed within *dg-ade6*+ when either *rrp1*+ or *rrp2*+ is over expressed appears independent of the presence of Swi6 and could be accounted for by spreading of the histone variant Cnp1 into that region that our Cnp1 ChIP data demonstrate (Fig. 2B).

We conclude that *rrp1*+ and *rrp2*+ are involved in modulating of nucleosome dynamics and that dysregulation of their copy number results in defects to centromere structure likely caused by misincorporation of Cnp1. This manifests as increased TBZ sensitivity, defects in transcriptional silencing and genetic instability.

Rrp1 and Rrp2 can bind to centromeric and/or telomeric regions

We have previously shown that Rrp1 and Rrp2 form foci co-localising with MMS-induced Rad52 foci at sites of DNA damage (Dziadkowiec et al., 2009; Dziadkowiec et al., 2013). Upon prolonged over-expression EGFP-tagged Rrp1 and Rrp2 bind to DNA and also form spontaneous foci in cells. Co-staining for EGFP-Rrp1 or EGFP-Rrp2 with Swi6-ECFP demonstrated that >40% of Rrp foci are formed in perinuclear regions and co-localise with Swi6 foci (Fig. 4A). This suggests that Rrp1 and Rrp2 can bind to centromeres and/or telomeres. However, Rrp1 and Rrp2 foci are formed in the absence of Swi6 and Clr4 (Fig. 4B) so Rrp1 and Rrp2 localisation is not dependent on heterochromatin. Interestingly, we observe that about 70% of Rrp1 and Rrp2 foci co-localise with Rad11 (Fig. 4C). What's

more, Rrp1 and Rrp2 also bind to fragmented DNA, as well as anaphase brigdes coated with Rad11. Some co-localising foci are also present within or at the boundaries of these structures (Fig. 4D). Such streches of DNA with foci can also be seen when Swi6-ECFP is used as a marker of chromatin (Fig. S3A). We thus propose that Rrp1 and Rrp2 bind to sites where spontaneous DNA damage and/or ssDNA accumulates in the genome and that the detrimental effect of their dysregulation is most pronounced at centromeres and/or telomeres.

While there are only an average of 1-2 molecules of RNA for Rrp1 and Rrp2 per cell (Quantitative gene expression, PomBase) and we are unable to detect these proteins when tagged at their native locus, ChIP of endogenously GFP-tagged Rrp1 and Rrp2 indicated their ability to associate with centromeres and telomeres (Fig. 4E). ChIP of over-expressed EGFP-tagged Rrp1 and Rrp2 shows that both proteins are enriched at centromeres and telomeres (Fig. S3B), consistent with Swi6 co-localisation data (Fig. 4A). However, when Rrp1 and Rrp2 are overproduced they are also likely to bind to chromatin across the genome, and thus their enrichment at these sites relative to actin control is modest.

Interdependence of *rrp1+* and *rrp2+* over-expression phenotypes

Previous genetic analysis of *rrp1*Δ and *rrp2*Δ cells in response to DNA damage demonstrated that these two proteins function as a unit in the HR response (Dziadkowiec et al., 2009). Here we observed differences between the two gene functions: upon *rrp2+* overexpression the growth defect is greater and the TBZ sensitivity and transcriptional repression are lower when compared to *rrp1+* over-expressing cells (Fig. 1A, 3B). Importantly, the growth defect, increased TBZ sensitivity and silencing caused by over-expression of *rrp1+* or *rrp2+* are not dependent on the presence of their respective paralogue (Fig. S4A). When both genes are over-expressed, the resulting growth defect is equivalent to that caused by over-expression of *rrp2+* (Fig. S4B). Furthermore, the increased toxicity of *rrp2+* as compared with *rrp1+* over-expression is partially dependent on the presence of the Rad51 recombinase (Fig. S4C). These data suggest the existence of separate roles for both proteins and imply that Rrp2 toxicity might also result from its activity at other loci than the centromere. Accordingly, recent work demonstrated an Rrp1-independent function for Rrp2 in regulating Top2 degradation (Wei et al., 2017). Thus, both Rrp1 and Rrp2 have activities that are independent of the other paralogue.

Disruption of centromere conferred by Rrp1 and Rrp2 overproduction depends differentially on their domains

Since Rrp1 and Rrp2 both have complex domain structures (Dziadkowiec et al., 2009) (Fig. 5A) we examined the importance of these domains. We chose the *swi6*Δ

background where the *rrp1*+ and *rrp2*+ copy number dysregulation induces growth defect comparable to *swi6*+, but where its effects on TBZ sensitivity and transcriptional repression of *dg-ade6*+ are more pronounced (Figs. 1A, 3B and S1C,D). First we confirmed that Rrp1 and Rrp2 with either Walker-B mutations (Rrp1-DAEA, Rrp2-DAEA), RING mutations (Rrp1-CS, Rrp2-CS) and Rrp2 with the 6 SIMs mutated (Rrp2-SIM) were all expressed (Fig. S5A). All the mutant proteins also form foci in the nucleus (Fig. S5B), albeit for Rrp1-DAEA their number is somewhat decreased, and all domains contribute to some extent to the loss of viability conferred by over-expression (Fig. S5C).

Over-expression of *rrp1-DAEA* or *rrp1-CS* did not cause marked growth defects or TBZ sensitivity (Fig. 5B), although only Rrp1-DAEA completely lost toxicity. Similarly, over-expression of *rrp1-DAEA* failed to increase transcriptional repression of *dg-ade6*+, while *rrp1-CS* showed an intermediate phenotype (Fig. 5B). For *rrp2*, no marked growth defect was observed when *rrp2-DAEA*, *rrp2-CS* or *rrp2-SIM* were over-expressed (Fig. 5C). Over-expression of all three allels resulted in a modest TBZ sensitivity and *rrp2-DAEA* and *rrp2-CS* over-expression resulted in intermediate levels of *dg-ade6*+ silencing. Thus, all three domains are involved in, but not critical for, proper centromere structure and function. Furthermore, the SIM domains, while important for TBZ sensitivity, do not significantly influence transcriptional repression (Fig. 5C).

These data indicate that, for Rrp1, its overexpression-induced growth defect and TBZ sensitivity are closely related to the disruption of centromere structure and depend on its putative translocase activity, but to a lesser extent on its RING domain. Conversely, for Rrp2 the growth defect and, to some extent, the TBZ sensitivity are not as closely related to disruption of centromere structure and differentially depend on separate Rrp2 activities. The differences between *rrp1*+ or *rrp2*+ over-expression phenotypes will be discussed later.

We next examined if the reduction of histone levels we observe after *rrp1*+ or *rrp2*+ over-expression was dependent on various domains of Rrp1 and Rrp2. Consistent with the results obtained from the TBZ sensitivity and silencing assays, only the potential translocase activity was required for Rrp1-induced H3 depletion, whereas the translocase and ubiquitin ligase activities were both required for Rrp2-induced H3 depletion (Fig. 6A,B). This is especially evident when the intensity of the H3 signal is normalized to the intensity of GFP signal (the tag on Rrp1 or Rrp2 protein) (Fig. 6C). This demonstrates that the differences in the amount of histone H3 we observe do not stem from the differences in wild type and mutant protein levels in transformants examined and indicates that the increase in Rrp1 or Rrp2 copy number destabilizes nucleosomes via translocase-dependent activities.

It has been reported in *S. cerevisiae* that global histone levels are reduced in cells exposed to genotoxic stress (Hauer et al., 2017). We observed similar effect in an *S. pombe* wild type strain and demonstrated that it is partially dependent on the presence of Rrp1 and

Rrp2 proteins (Fig. 6D,E). These observations are consistent with results obtained for *rrp1*+ or *rrp2*+ over-expression (Fig. 6A,B) and lend support to a role for Rrp1 and Rrp2 in regulating nucleosome dynamics. Interestingly, we did not detect any defect in global regular spacing of nucleosomes in cells over-expressing *rrp1*+ or *rrp2*+ using an MNase ladder assay (Fig. S6). This is reminiscent of what was reported for *S. pombe* mutants devoid of the CHD1 chromatin remodelers that also didn't exhibit alterations in global nucleosome spacing by MNase assay (Pointner et al., 2012; Walfridsson et al., 2007). This aspect of Rrp1 and Rrp2 activity deserves further future exploration.

Rrp2 acts at telomeres to regulate Top2

Over-expression of *rrp2*+ generates more pronounced cell toxicity than *rrp1*+ (Fig. 1A, S4C) and the growth defect caused by rrp2+ over-expression can be uncoupled from centromeric transcription silencing (Fig. 5C). Rrp2 overproduction has been shown to result in the accumulation of high-molecular-weight (HMW) SUMO conjugates (Nie et al., 2017). We also observed this accumulation and show it is specific for *rrp2*+ and not *rrp1*+ over-expression (Fig. 7A). Previous work has demonstrated that Rrp2 functions to protect Top2 from premature degradation by preventing access of STUbLs (Wei et al., 2017), a role that requires its translocase and SUMO binding activities. At telomeres it has been demonstrated that *top2* mutants can alleviate the growth defect at low temperatures associated with Taz1 loss (Germe et al., 2009). *taz1*Δ cells are cold sensitive due to aberrant telomere replication which results in telomere entanglements that cause chromosome bridges during mitosis. In addition to *top2* mutants, a reduction in the levels of HMW SUMO conjugates (Nie et al., 2017; Rog et al., 2009) also rescues *taz1*Δ cold sensitivity. Taken together, these data may explain the differential toxicity observed when over-expressing *rrp2*+ compared to *rrp1*+.

Consistent with this hypothesis, *taz1*Δ*rrp2*Δ but not *taz1*Δ*rrp1*Δ double mutants grow well at low temperature (Fig. 7B), with viability comparable to that of *taz1*Δ*nmt81-ulp1* cells (Fig. 7B, C). Over-expression of Ulp1 SUMO protease has previously been reported to reduce SUMO chains and rescue *taz1*Δ cold sensitivity (Rog et al., 2009). *rrp2*Δ also reversed the characteristic *taz1*Δ mitotic defects: anaphase bridges, "pointing finger" structures, chromosome missegregation events (Fig. 7D) and systemic checkpoint activation resulting in cell elongation (Fig. 7E). If the interaction of Rrp2 with Top2 is involved in the role of Rrp2 at telomeres, it would be predicted that *taz1*Δ toxicity would be dependent on the Rrp2 SUMO interaction and translocase activities, but not on a functional RING domain (Wei et al., 2017) (see Discussion). Over-expressing *rrp2*+ in the *taz1*Δ*rrp2*Δ mutant restored cold sensitivity as expected. In contrast, over-expressing *rrp2-DAE*A or *rrp2-SIM* did not, whereas over-expression of *rrp2-CS* phenocopied *rrp2*+ (Fig. 7F).

We conclude that the improper processing of telomere replication intermediates, which is distinct from the effects of Rrp2 at centromeres, is the likely source of the increased Rrp2 overproduction-induced growth defect when compared to Rrp1.

DISCUSSION

Rrp1 and Rrp2 are orthologues of *S. cerevisiae* Uls1, a DNA translocase and STUbL. Our previous work has shown that Rrp1 and Rrp2 work as an inter-dependent unit in a sub-pathway of Rad51-dependent homologous recombination (Dziadkowiec et al., 2009; Dziadkowiec et al., 2013). Rrp2 also has a separate Rrp1-independent function in protecting Top2 from STUbL-mediated degradation (Wei et al., 2017) and has been implicated in the regulation of meiotic recombination hotspot activity (Storey et al., 2018). The phenotypes of *rrp1* and *rrp2* null mutants are generally subtle, often requiring concomitant deletion of other genes before they can be detected. We thus chose to over-express the proteins because this can reveal informative phenotypes. We found that over-expression of either *rrp1+* or *rrp2+* impaired chromosome segregation and resulted in viability loss. Over-expressed Rrp1 and Rrp2 formed foci that frequently colocalised with Swi6, suggesting an association with heterochromatin that is correlated with centromeres and telomeres in *S. pombe*. Indeed we found that Rrp1 and Rrp2 were enriched at both centromeres and telomeres by ChIP analysis.

Rrp1 and Rrp2 can modulate centromere structure and function

Chromosome instability and lagging mitotic chromosomes can result from aberrant centromere chromatin structure (Maruyama et al., 2006).

While *rrp1+* or *rrp2+* over-expression did not have marked effects on TBZ sensitivity in wildtype cells, *rrp1+* over-expression (and to a lesser extent *rrp2+* over-expression) significantly increased the TBZ sensitivity of *swi6*Δ cells. This implied that correct regulation of Rrp1 and Rrp2 function becomes especially important when centromere structure is disturbed. Centromeric nucleosome localisation has been shown to be important for maintaining centromere function in *S. pombe* and *S. cerevisiae* (Castillo et al., 2007; Hildebrand and Biggins, 2016). We thus reasoned that the TBZ sensitivity may, at least in part, be caused by perturbed centromere structure resulting from Cnp1 mislocalisation. Indeed we found that *rrp1+* or *rrp2+* over-expression lead to an increase in Cnp1 ChIP signal at *cnt* and Cnp1 spreading into the into *dg* repeat regions from which it is normally excluded.

Interestingly, when we tested for the epigenetic regulation of transcription at the centromere we found that *rrp1+* and *rrp2+* over-expression increased silencing of a *dg-ade6+* gene in wildtype cells and that *rrp1+* and, to a lesser degree, *rrp2+* over-expression reversed the de-repression of *dg-ade6+* that is conferred by *swi6+* deletion. Thus *rrp1+* or *rrp2+* over-expression acts to decrease transcription of *dg-ade6+* in a manner that does not

require Swi6. This would be consistent with previous reports that misincorporation of CENP-A can lead to transcriptional defects (Hildebrand and Biggins, 2016). We did not observe a global change of Cnp1 levels in *rrp1+* and *rrp2+* over-expressing cells but saw a reduction in histone H3 levels. This gives rise to an increased Cnp1 : H3 ratio. H3 and Cnp1 compete for incorporation into chromatin and their relative amounts are important for proper Cnp1 centromeric localisation (Choi et al., 2012). We thus propose that Rrp1 and Rrp2 influence centromere structure by indirect modulation of canonical nucleosomes. Future studies will be important to identify how Rrp1 and Rrp2 work with other chromatin remodelling factors that have well-established roles in maintaining the appropriate histone levels and ensuring proper Cnp1 localisation (Choi et al., 2017; Prasad and Ekwall, 2011; Strålfors et al., 2011; Walfridsson et al., 2007).

The depletion of global histone levels, dependent on the INO80 nucleosome remodeler, has recently been demonstrated in *S. cerevisiae* to play a role in the DNA damage response (Hauer et al., 2017). We also found that global histone levels were reduced in *S. pombe* after genotoxic stress and this was partly dependent on Rrp1 and Rrp2. It is thus possible that, through the regulation of nucleosome dynamics, Rrp1 and Rrp2 modulate the actions of repair pathways at sites of DNA damage or arrested replication forks.

This could potentially explain the role of Rrp1 and Rrp2 in the Swi5-Sfr1 sub-pathway of HR (Dziadkowiec et al, 2013). In this context it is important to note that Rad51 and Rad54 have been shown to promote intra-chromatid recombination between centromere repeats that is crucial for the integrity of centromeric chromatin. However, Rad54 has also been found to have a Rad51-independent function in centromere maintenance that required its chromatin remodelling activity (Onaka et al., 2016). Thus, Rrp1 and Rrp2 might act within an HR pathway but also function as chromatin remodelers and regulate histone dynamics in a variety of different contexts and circumstances. Lending support to this conjecture, Rrp2 was recently identified together with Hip1 (histone chaperone), Ino80 complex subunits and the nucleosome evictor Fft3 (Fun30) as a factor contributing to recombination hotspot activation during meiosis via a process that is proposed (Storey et al., 2018) to involve the exchange of individual histone subunits.

Rrp2 has an independent role at telomeres

rrp2+ over-expression leads to greater cell toxicity than *rrp1+* over-expression. However, the TBZ sensitivity of cells over-expressing *rrp2+* was lower than that induced by *rrp1+* over-expression. Furthermore, the loss of viability caused by *rrp2+* over-expression, unlike for *rrp1+* over-expression, is Rad51-dependent. Thus, the growth defect induced by *rrp2+* over-expression can be partially separated from its role in centromere structure, demonstrating that Rrp2 has additional function(s) when over-expressed. It has recently been shown that Rrp2, but not Rrp1, protects cells from Top2-induced DNA damage (Wei et

al., 2017). Based on these data and the role of Top2 and SUMO in telomere replication in *taz1*Δ mutants (Rog et al., 2009), we hypothesized that Rrp2, but not Rrp1, is involved in telomere maintenance. In support of this, we showed that deletion of *rrp2*+, but not of *rrp1*+, reversed *taz1*Δ mitotic defects. We also showed that Rrp2 SUMO binding and translocase activities were necessary for Rrp2 toxicity in the *taz1*Δ mutant background. We thus propose that the recently described interaction with Top2 (Wei et al., 2017) underpins the role of Rrp2 at the telomeres: in *rrp2*Δ mutants Top2 is not protected from STUbL degradation and this increases the probability of exposing a DSB if Top2 is degraded while still at the Top2cc stage (Wei et al., 2017). Similarly, the *top2-191* mutant (Germe et al., 2009), which is trapped longer at the Top2cc stage during catalytic cycle, intrinsically faces higher risk of being inadvertently degraded by STUbL, thus exposing DNA breaks. While this outcome is generally best avoided in otherwise wild type cells, in *taz1*Δ (where telomere separation during anaphase is hindered by entanglement) introducing breaks into telomeric DNA likely allows the separation of the chromosomes. This would prevent chromosome arm breakage due to incomplete DNA segregation and subsequent septation in *taz1*Δ mutant and thus lead to the rescue of the *taz1*Δ growth defect seen in both *top2-191* (Germe et al., 2009) and *rrp2*Δ background.

Conclusion

Taken together our data show that Rrp1 and Rrp2 help to ensure genetic stability by modulating histone levels. These functions are important at repetitive difficult-to-replicate regions of the genome, suggesting they respond to replication associated intrinsic DNA damage.

MATERIALS AND METHODS

Yeast strains, plasmids and general methods

Strains and plasmids used in this study are listed in Tables S1 and S2, respectively. Media used for *S. pombe* growth were as described (Moreno et al., 1991). Yeast cells were cultured at 28°C in complete yeast extract plus supplements (YES) medium or glutamate-supplemented Edinburgh minimal medium (EMM). Thiamine was added where required (5 µg/mL), as were geneticin (ICN Biomedicals) (100 µg/mL), nurseotricin (Werner Bioagents) (200 µg/mL) and hygromycin (Sigma-Aldrich). For YES low ade plates, the concentration of adenine was reduced 10-fold. pREP81-FLAG vector and plasmids carrying wild type and mutated forms of *rrp1*$^{+}$ and *rrp2*$^{+}$ were constructed using Gibson Assembly Cloning Method/ Gibson Assembly® Cloning Kit (NEB). All primers used to amplify gene sequences by PCR are listed in Table S3. Amplified fragments were cloned into NdeI and BamHI digested pREP81 vector. After Gibson cloning inserts were cut by NdeI and SmaI

digestion and cloned into pREP41-EGFP plasmid. Plasmid over-expressing *rrp2-SIM* was obtained by cloning a *rrp2*+ coding sequence from pDUAL-Prrp2-GFP-Rrp2-SIM(1-6)*, a gift from Li Lin Du (Wei et al., 2017) into pREP41-EGFP.

Whole protein extract analysis

Protein extracts were prepared by the trichloroacetic acid (TCA) method. Briefly, after 24 hour of induction of *nmt* promoter by removal of thiamine from media, mid-logarithmic cells (~10^8) of indicated strains were harvested and lysed with lysis buffer (2 M NaOH, 7% β-mercaptoethanol). Total protein was precipitated by adding 50% TCA. Pellet was then resuspended in 1 M Tris at pH 8 and 4x Laemmli buffer was added (250 mM Tris-HCl, pH 6.8, 8% SDS, 20% glycerol, 0.02% Bromophenol blue, 7% β-mercaptoethanol). Obtained samples were analysed by SDS-PAGE and Western blotting using anti-GFP (Roche, 11814460001), anti-FLAG (Sigma-Aldrich, F1804), anti-H3 (Abcam, ab1791) or anti-GAPDH (loading control, Invitrogen, MA5-15738) antibodies. Blotted membranes were stained with the Ponceau S (Sigma-Aldrich) to detect total proteins. For protein quantification Image Lab (Western blots) or ImageJ software (Ponceau S staining) was used. Relative intensity was calculated by dividing sample intensities by the mean of control intensities obtained for each blot (details for each experiment are provided in figure captions). For each experiment data from two different transformants from two independent protein isolations were analysed.

Detection of high-molecular weight SUMO conjugates

Protein extracts for identifying high-molecular weight SUMO-conjugates were prepared according to (Nie et al., 2017) with following modifications. After 24 hour induction of *nmt* promoter by removal of thiamine from media, mid-log cells (~2×10^8) were washed with STOP buffer (10 mM EDTA, 50 mM NaF, 150 mM NaCl) and pellets were frozen in liquid nitrogen. Cells were resuspended in 200 µL of 20% TCA with 200 µL of glass beads (Roth) and subsequently disrupted by bead beating. Next, 400 µL of 5% TCA was added, lysate was separated from the beads and centrifuged at 16,000 *g* for 5 min at 4°C. The pellet was washed twice with 0.1% TCA. The precipitated proteins were resuspended in 8 M urea, 50 mM Tris, pH 8.5, 150 mM NaCl. After estimation of protein concentration by measurement of absorbance at 280 nm, 2x loading buffer was added (6 M urea, 62.5 mM Tris-HCl pH 6.8, 2% SDS, 20% glycerol, 0.01% bromophenol blue, 3.5% β-mercaptoethanol) and samples were analysed by SDS-PAGE using 4-20% gradient Mini Protean TGX Precast Gel (Bio-Rad). Membrane was visualized for total protein with Ponceau S (Sigma-Aldrich) and Western blot was performed using anti-Pmt3 polyclonal serum (gift from Felicity Watts).

Spot assays

Cells were grown to mid-log phase, then serially diluted by 10-fold and 2 µL aliquots were spotted onto relevant plates (YES or EMM) without drug or plates containing thiabendazole (TBZ). Plates were incubated for 3-5 days in 28°C (unless stated otherwise)

and photographed. All assays were repeated at least twice. TBZ was added to the plates at the concentrations.

Survival assay

Cells were grown for 48 hours in minimal medium with (repressed conditions) or without thiamine (over-expression) at 28°C. 500 µL aliquots were collected, serially diluted and plated onto YES plates to determine the number of viable cells. Plates were incubated for 3-5 days at 28°C. The viable cells were counted and percentage of survival was calculated. For temperature survival, cells were grown to mid-log phase in rich medium in 28°C or 20°C. Samples were collected and diluted in the same way as above, plated onto YES plates and incubated for 3-5 days at 28°C. The percentage of survival in 20°C was calculated against the 28°C control.

Chromosome loss

Indicated strains where streaked to single colonies on EMM low Ade plates (adenine concentration reduced to 7.5 mg/L) with thiamine and a single white colony was inoculated in EMM without thiamine and incubated for 48 h at 28°C. Then cultures were appropriately diluted, plated on YES low Ade plates and incubated for 3-4 days at 28°C. Percentage of red to white colonies was then calculated.

Fluorescence microscopy

To determine the foci formation of Rrp1 and Rrp2 proteins, their co-localisation with Swi6 protein and Rad11 appropriate strains were grown for 24 h in EMM medium without thiamine. 1 mL of culture was harvested, washed with water and subjected to fluorescent microscopy analysis. For Rrp1 and Rrp2 foci images were captured under 100x magnification using Axio Imager A.2 (Carl Zeiss) with Canon digital camera, and analysed with Axiovision rel. 4.8. For co-localisation experiments, data were collected under 63x magnification with confocal microscope Leica TCS SP8 (Leica Microsystems) equipped with Leica HyD SP detector, and analysed with LAS X 3.3.0.

For examination of mitotic defects induced by *rrp1*$^{+}$ or *rrp2*$^{+}$ over-expression samples taken from cultures grown for 48 hours in EMM medium without thiamine. were washed and fixed in 70% ethanol. After rehydration, cells were stained with 1 mg/mL 4',6-diamidino-2-phenylindole (DAPI) and 1 mg/mL p-phenylenediamine in 50% glycerol and examined by fluorescence microscopy with Axio Imager A.2 (Carl Zeiss).

To observe Cnp1-CFP and Rad11-GFP foci in rrp1+ or rrp2+ over-expressing cells transformants were grown to mid-logarithmic phase in EMM without thiamine. Cells were then centrifuged and resuspended in 1 mL of fresh EMM. A drop of 1 µL was spotted on the layer of 1.4% agarose in filtered EMM covering a Thermo Scientific slide (ER-201B-CE24). 14 z-stack pictures (each z step of 300 nm) for Cnp1-CFP were captured using a 3D microscope (LEICA DMRXA) equipped with a CoolSNAP monochromic camera (Roper

Scientific) under 100X magnification, exposure time for CFP 750 ms, with METAMORPH software. For Rad11-GFP 14 z-stack pictures (each z step of 300 nm), exposed for 100 ms, were captured using a Nikon inverted microscope equipped with the Perfect Focus System, a 100X/1.45-NA PlanApo oil immersion objective, Yokogawa CSUX1 confocal unit, Photometrics Evolve512 EM-CCD camera and a laser bench (Errol) with 491 nm diode laser, 100 mX (Cobolt) at 20% of laser power using METAMORPH software. Images were z-projected and analysis was performed using ImageJ software. Image acquisition with LEICA DMRXA 3D microscope and Nikon inverted microscope were performed on the PICT-IBiSA Orsay Imaging facility of the Institut Curie.

Histone loss upon DNA damage treatment

Cultures of wild type and mutant cells were grown in YES at 28°C to OD 0.4-0.7 and split into two tubes. 12 mM HU and 20 µM CPT was added to one tube (the other serving as an untreated control) and incubation continued at 28°C for 4 hours. Total protein was then isolated and subjected to Western blot analysis.

Chromatin immunoprecipitation (ChIP)

Experiments were performed as described in (Ait Saada et al., 2017) with small modifications. Briefly, yeast cultures were grown to logarithmic phase in YES medium or for 24 hours in EMM medium without thiamine and 10^9 cells were pelleted and resuspended in PBS with 2.5 mg/ml DMA with 0.25% DMSO and incubated 45 min with shaking at RT. Cells were pelleted, washed with PBS and incubated with 1% formaldehyde for another 15 min. Glycine was added to neutralize formaldehyde. Cells were then pelleted, washed with PBS, frozen in liquid nitrogen and stored at -80˚C. After disrupting cells by bead beating in ChIP lysis buffer (50 mM HEPES pH 7.4; 140 mM NaCl; 1 % Triton X100; 0.1% Na-deoxycholate) with PMSF (1 mM) and protease inhibitor (Complete EDTA –free protease inhibitor cocktail, Roche) 10 cycles of sonication were performed: 20 seconds ON and 60 seconds on ice using water ultrasonicator (LABART). Before immunoprecipitation, input samples were taken as a control, then anti-GFP antibody (Life Technologies, A-11122) was added to each sample. Samples were incubated for 1 h at 4°C, after that 20 µL of Dynabeads Protein G (Thermo Fisher) was added per sample and incubated over night at 4°C. After washing steps and de-crosslink for 2 h at 65°C DNA was recovered by ethanol precipitation. Purified DNA was subjected to further analyses by qPCR using StepOne (Thermo Fisher) thermocycler. Target and control (actin) primers used are listed in Table S3.

Data were collected from at least one qPCR performed on DNA from four independent biological experiments. The Ct value (number of cycles required for the fluorescent signal to cross the threshold) from input samples ($Ct_{(IN)}$) and ChIP samples ($Ct_{(ChIP)}$) was recorded by StepOne Software. Following formula was used to calculate

percent enrichment of the amount of protein binding to a target locus over actin: $(100\times(1/2\text{^}(Ct_{(ChIP)}\text{-}Ct_{(IN)}))_{target}/(100\times(1/2\text{^}(Ct_{(ChIP)}\text{-}Ct_{(IN)}))_{actin}$.

MNase digestion

The MNase ladder assay was performed according to (Lantermann et al., 2009). After 24 hour induction of *nmt* promoter by removal of thiamine, mid-log cells were crosslinked with 0.5% formaldehyde for 20 minutes. Cell wall was removed by digestion with Zymolase T100 in S buffer (50 mM Tris-HCl pH 7.4, 1 M sorbitol, 10 mM 2-mercaptoethanol) for 1 h. Spheroplasts were resuspended in NP buffer (1 M sorbitol, 50 mM Tris-HCl pH 7.4, 5 mM $MgCl_2$, 1 mM $CaCl_2$, 0.75% NP-40) and divided into 100 µl samples. Micrococcal nuclease (Sigma-Aldrich) was added to samples to the final concentration of 5 U/ml and, after incubation for indicated times, the reaction was stopped by the addition of buffer containing 0.35 M EDTA, 3% SDS, and 1.5 mg/ml proteinase K. Digested DNA was isolated using phenol:chloroform:isoamyl alcohol, washed with ethanol, gently resuspended in MQ water and treated with 0.01 mg/ml RNAseA (Sigma-Aldrich) for 30 minutes in 37°C. Samples were run on 1.5% agarose gel in TAE buffer. Bands were visualized by SimplySafe staining.

Statistical data analysis

In all box and whiskers plots boxes represent the range from 25 to 75%, whiskers—the range from 5 to 95%, lines dividing the boxes—the median and full squares—the mean value. The error bars represent the standard deviation about the mean values. Student's t-test was used to calculate the P-values (* $0.01 < \text{P-value} \leq 0.05$, ** $0.001 < \text{P-value} \leq 0.01$, *** $\text{P-value} \leq 0.001$).

FUNDING

This work was supported by the grant from The National Science Centre, Poland, http://ncn.gov.pl (Harmonia 5, 2013/10/M/NZ1/00254) to DD. The funders had no role in study design, data collection and analysis, decision to publish, or preparation of the manuscript.

ACKNOWLEDGMENTS

We thank Robin Allshire, Julie Cooper, Jo Murray, Susan Forsburg, Hiroshi Iwasaki and Benoit Arcangioli for providing strains, Nick Boddy and Minghua Nie for strains and sharing the protocol for isolation of SUMOylated proteins, Felicity Watts for the kind gift of strains and anti-Pmt3 serum and Wojciech Białek for reagents. We thank Natalia Trempolec and Joanna Morcinek-Orłowska for involvement in the initial stages of this project. We are grateful to Li Lin Du for sharing unpublished data and providing Rrp2 and Rrp2-SIM plasmids, and to Sarah Lambert for comments on the manuscript and hosting Kamila for a research project in her laboratory.

REFERENCES

Ait Saada, A., Teixeira-Silva, A., Iraqui, I., Costes, A., Hardy, J., Paoletti, G., Fréon, K. and Lambert, S. (2017). Unprotected Replication Forks Are Converted into Mitotic Sister Chromatid Bridges. *Mol. Cell* **66**, 398–410.

Akamatsu, Y., Tsutsui, Y., Morishita, T., Siddique, M. S. P., Kurokawa, Y., Ikeguchi, M., Yamao, F., Arcangioli, B. and Iwasaki, H. (2007). Fission yeast Swi5/Sfr1 and Rhp55/Rhp57 differentially regulate Rhp51-dependent recombination outcomes. *EMBO J.* **26**, 1352–1362.

Allshire, R. C., Nimmo, E. R., Ekwall, K., Javerzat, J. P. and Cranston, G. (1995). Mutations derepressing silent centromeric domains in fission yeast disrupt chromosome segregation. *Genes Dev.* **9**, 218–33.

Castillo, A. G., Mellonea, B. G., Partridgeb, J. F., Richardsonc, W., Hamilton, G. L., Allshire, R. C. and Pidoux, A. L. (2007). Plasticity of fission yeast CENP-A chromatin driven by relative levels of histone H3 and H4. *PLoS Genet.* **3**, 1264–1274.

Choi, E. S., Strålfors, A., Catania, S., Castillo, A. G., Svensson, J. P., Pidoux, A. L., Ekwall, K. and Allshire, R. C. (2012). Factors That Promote H3 Chromatin Integrity during Transcription Prevent Promiscuous Deposition of CENP-ACnp1 in Fission Yeast. *PLoS Genet.* **8**, e1002985.

Choi, E. S., Cheon, Y., Kang, K. and Lee, D. (2017). The Ino80 complex mediates epigenetic centromere propagation via active removal of histone H3. *Nat. Commun.* **8**, 529.

Dziadkowiec, D., Petters, E., Dyjankiewicz, A., Karpiński, P., Garcia, V., Watson, A. T. and Carr, A. M. (2009). The role of novel genes rrp1(+) and rrp2(+) in the repair of DNA damage in Schizosaccharomyces pombe. *DNA Repair (Amst).* **8**, 627–636.

Dziadkowiec, D., Kramarz, K., Kanik, K., Wiśniewski, P. and Carr, A. M. (2013). Involvement of Schizosaccharomyces pombe rrp1+ and rrp2 + in the Srs2- and Swi5/Sfr1-dependent pathway in response to DNA damage and replication inhibition. *Nucleic Acids Res.* **41**, 8196–8209.

Ekwall, K., Nimmo, E. R., Javerzat, J. P., Borgstrøm, B., Egel, R., Cranston, G. and Allshire, R. C. (1996). Mutations in the fission yeast silencing factors clr4+ and rik1+ disrupt the localisation of the chromo domain protein Swi6p and impair centromere function. *J. Cell Sci.* **109**, 2637–48.

Germe, T., Miller, K. and Cooper, J. P. (2009). A non-canonical function of topoisomerase II in disentangling dysfunctional telomeres. *EMBO J.* **28**, 2803–2811.

Gonzalez, M., He, H., Dong, Q., Sun, S. and Li, F. (2014). Ectopic centromere nucleation by CENP-A in fission yeast. *Genetics* **198**, 1433–1446.

Hauer, M. H., Seeber, A., Singh, V., Thierry, R., Sack, R., Amitai, A., Kryzhanovska, M., Eglinger, J., Holcman, D., Owen-Hughes, T., et al. (2017). Histone degradation in response to DNA damage enhances chromatin dynamics and recombination rates. *Nat. Struct. Mol. Biol.* **24**, 99–107.

Hildebrand, E. M. and Biggins, S. (2016). Regulation of Budding Yeast CENP-A levels Prevents Misincorporation at Promoter Nucleosomes and Transcriptional Defects. *PLOS Genet.* **12**, e1005930.

Horigome, C., Bustard, D. E., Marcomini, I., Delgoshaie, N., Tsai-Pflugfelder, M., Cobb, J. A. and Gasser, S. M. (2016). PolySUMOylation by Siz2 and Mms21 triggers relocation of DNA breaks to nuclear pores through the Slx5/Slx8 STUbL. *Genes Dev.* **30**, 931–945.

Lambert, S., Watson, A. T., Sheedy, D. M., Martin, B. and Carr, A. M. (2005). Gross chromosomal rearrangements and elevated recombination at an inducible site-specific replication fork barrier. *Cell* **121**, 689–702.

Lantermann, A., Strålfors, A., Fagerström-Billai, F., Korber, P. and Ekwall, K. (2009). Genome-wide mapping of nucleosome positions in Schizosaccharomyces pombe. *Methods* **48**, 218–25.

Lescasse, R., Pobiega, S., Callebaut, I. and Marcand, S. (2013). End-joining inhibition at telomeres requires the translocase and polySUMO-dependent ubiquitin ligase Uls1. *EMBO J.* **32**, 805–815.

Li, P. C., Petreaca, R. C., Jensen, A., Yuan, J. P., Green, M. D. and Forsburg, S. L. (2013). Replication Fork Stability Is Essential for the Maintenance of Centromere Integrity in the Absence of Heterochromatin. *Cell Rep.* **3**, 638–645.

Marcomini, I., Shimada, K., Delgoshaie, N., Horigome, C., Naumann, U., Gasser, S. M., Marcomini, I., Shimada, K., Delgoshaie, N., Yamamoto, I., et al. (2018). Asymmetric Processing of DNA Ends at a Double- Strand Break Leads to Unconstrained Dynamics and Article Asymmetric Processing of DNA Ends at a Double-Strand Break Leads to Unconstrained Dynamics and Ectopic Translocation. *CellReports* **24**, 2614-2628.e4.

Maruyama, T., Nakamura, T., Hayashi, T. and Yanagida, M. (2006). Histone H2B mutations in inner region affect ubiquitination, centromere function, silencing and chromosome segregation. *EMBO J.* **25**, 2420–2431.

McGlynn, P. and Lloyd, R. G. (2002). Recombinational repair and restart of damaged replication forks. *Nat. Rev. Mol. Cell Biol.* **3**, 859–70.

Mejia-Ramirez, E., Limbo, O., Langerak, P. and Russell, P. (2015). Critical Function of γH2A in S-Phase. *PLOS Genet.* **11**, e1005517.

Miller, K. M. and Cooper, J. P. (2003). The telomere protein Taz1 is required to prevent and repair genomic DNA breaks. *Mol. Cell* **11**, 303–13.

Miller, K. M., Ferreira, M. G. and Cooper, J. P. (2005). Taz1, Rap1 and Rif1 act both interdependently and independently to maintain telomeres. *EMBO J.* **24**, 3128–35.

Mizuno, K., Miyabe, I., Schalbetter, S. a, Carr, A. M. and Murray, J. M. (2013). Recombination-restarted replication makes inverted chromosome fusions at inverted repeats. *Nature* **493**, 246–9.

Moreno, S., Klar, A. and Nurse, P. (1991). Molecular genetic analysis of fission yeast Schizosaccharomyces pombe. *Methods Enzymol.* **194**, 795–823.

Murray, J. M., Tavassoli, M., Al-Harithy, R., Sheldrick, K. S., Lehmann, A. R., Carr, A. M. and Watts, F. Z. (1994). Structural and functional conservation of the human homolog of the Schizosaccharomyces pombe rad2 gene, which is required for chromosome segregation and recovery from DNA damage. *Mol. Cell. Biol.* **14**, 4878–88.

Nakamura, K., Okamoto, A., Katou, Y., Yadani, C., Shitanda, T., Kaweeteerawat, C., Takahashi, T. S., Itoh, T., Shirahige, K., Masukata, H., et al. (2008). Rad51 suppresses gross chromosomal rearrangement at centromere in Schizosaccharomyces pombe. *EMBO J.* **27**, 3036–3046.

Nie, M., Moser, B. A., Nakamura, T. M. and Boddy, M. N. (2017). SUMO-targeted ubiquitin ligase activity can either suppress or promote genome instability, depending on the nature of the DNA lesion. *PLOS Genet.* **13**, e1006776.

Olson, H. C., Davis, L., Kiianitsa, K., Khoo, K. J., Liu, Y., Knijnenburg, T. A. and Maizels, N. (2018). Increased levels of RECQ5 shift DNA repair from canonical to alternative pathways. *Nucleic Acids Res.* **46**, 9496–9509.

Onaka, A. T., Toyofuku, N., Inoue, T., Okita, A. K., Sagawa, M., Su, J., Shitanda, T., Matsuyama, R., Zafar, F., Takahashi, T. S., et al. (2016). Rad51 and Rad54 promote noncrossover recombination between centromere repeats on the same chromatid to prevent isochromosome formation. *Nucleic Acids Res.* **44**, 10744–10757.

Pointner, J., Persson, J., Prasad, P., Norman-Axelsson, U., Strålfors, A., Khorosjutina, O., Krietenstein, N., Peter Svensson, J., Ekwall, K. and Korber, P. (2012). CHD1 remodelers regulate nucleosome spacing in vitro and align nucleosomal arrays over gene coding regions in S. pombe. *Embo J.* **31**, 4388–4403.

Prasad, P. and Ekwall, K. (2011). New insights into how chromatin remodellers direct CENP-A to centromeres. *EMBO J.* **30**, 1875–6.

Rog, O., Miller, K. M., Ferreira, M. G. and Cooper, J. P. (2009). Sumoylation of RecQ Helicase Controls the Fate of Dysfunctional Telomeres. *Mol. Cell* **33**, 559–569.

Schlacher, K., Christ, N., Siaud, N., Egashira, A., Wu, H. and Jasin, M. (2011). Double-strand break repair-independent role for BRCA2 in blocking stalled replication fork degradation by MRE11. *Cell* **145**, 529–42.

Sfeir, A., Kosiyatrakul, S. T., Hockemeyer, D., MacRae, S. L., Karlseder, J., Schildkraut, C. L. and de Lange, T. (2009). Mammalian telomeres resemble fragile sites and require TRF1 for efficient replication. *Cell* **138**, 90–103.

Storey, A. J., Wang, H.-P., Protacio, R. U., Davidson, M. K., Tackett, A. J. and Wahls, W. P. (2018). Chromatin-mediated regulators of meiotic recombination revealed by proteomics of a recombination hotspot. *Epigenetics Chromatin* **11**, 64.

Strålfors, A., Walfridsson, J., Bhuiyan, H. and Ekwall, K. (2011). The FUN30 Chromatin Remodeler, Fft3, Protects Centromeric and Subtelomeric Domains from Euchromatin Formation. *PLoS Genet.* **7**, e1001334.

Swanston, A., Zabrady, K. and Ferreira, H. C. (2019). The ATP-dependent chromatin remodelling enzyme Uls1 prevents Topoisomerase II poisoning. *Nucleic Acids Res.* **47**, 6172–6183.

Walfridsson, J., Khorosjutina, O., Matikainen, P., Gustafsson, C. M. and Ekwall, K. (2007). A genome-wide role for CHD remodelling factors and Nap1 in nucleosome disassembly. *EMBO J.* **26**, 2868–79.

Wei, Y., Diao, L.-X., Lu, S., Wang, H.-T., Suo, F., Dong, M.-Q. and Du, L.-L. (2017). SUMO-Targeted DNA Translocase Rrp2 Protects the Genome from Top2-Induced DNA Damage. *Mol. Cell* **66**, 581–596.

Yuan, J. and Chen, J. (2011). The role of the human SWI5-MEI5 complex in homologous recombination repair. *J. Biol. Chem.* **286**, 9888–93.

Figures

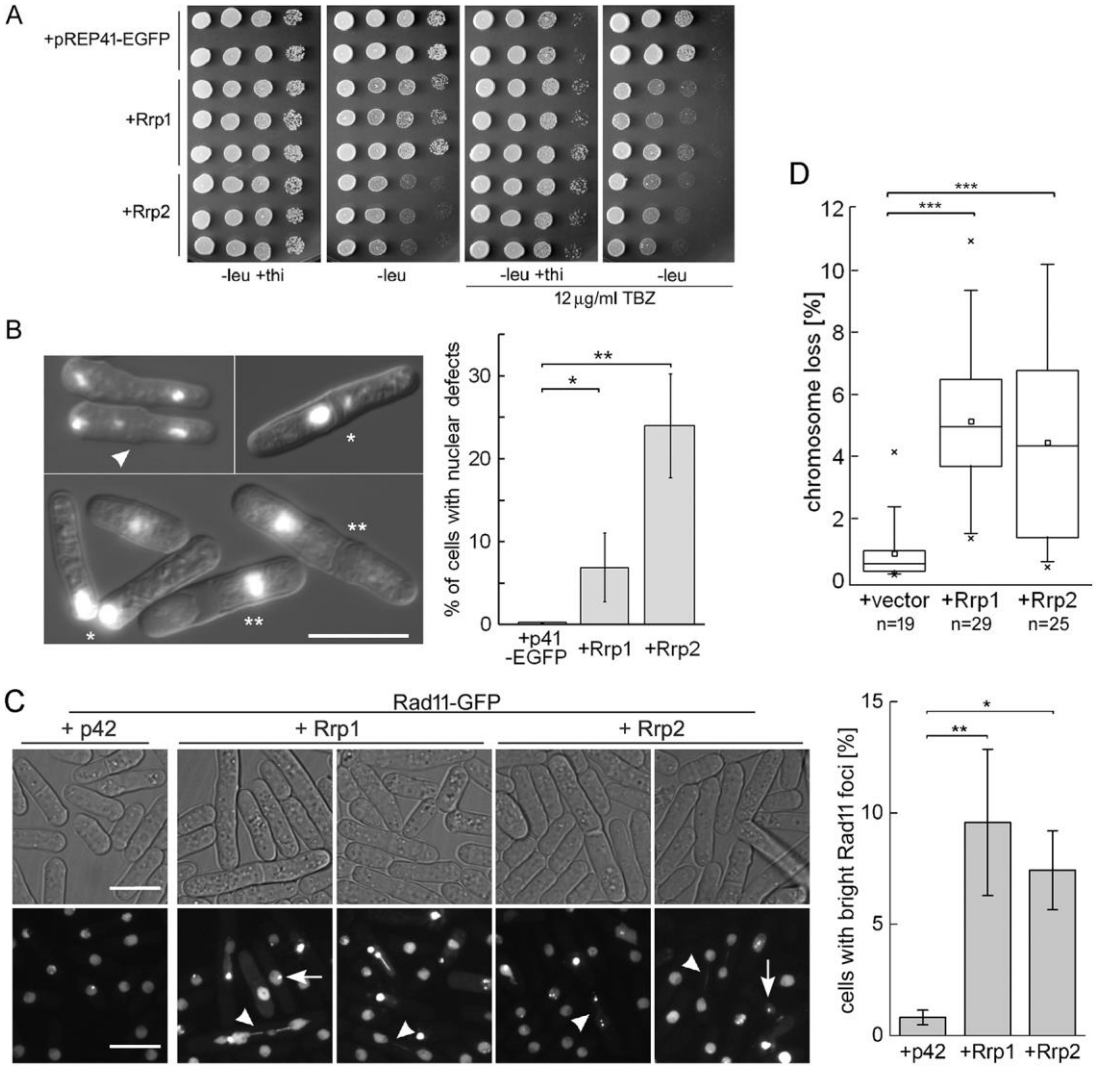

Figure 1 Up regulation of Rrp1 and Rrp2 level leads to chromosome instability

Induction of *rrp1+* or *rrp2+* expression results in (A) growth defect and increase in TBZ sensitivity determined by spot test analysis, with TBZ added to the plates at the indicated concentration, (B) mitotic aberrations, such as lagging/stretched chromosomes/anaphase bridges (marked with white arrowhead), cut (marked as *) and non-disjunction (marked as **) as observed by DAPI staining of the nuclei. 5 independent transformants for vector, *rrp1+* or *rrp2+* were analysed and the total number of cells counted was above 1000. Scale bar represents 10 µm. (C) Bright Rad11 foci (representative examples marked with white arrows) and Rad11 coated DNA bridges (marked with white arrowhead) accumulate in *rrp1+* or *rrp2+* over-expressing cells. Regular Rad11 foci are unmarked. The experiment was repeated 3 times and the total number of cells counted was above 2000. Scale bar represents 10 µm. (D) Induction of *rrp1+* or *rrp2+* expression leads to the loss of the

nonessential Ch^{16} minichromosome carrying the *ade6-216* allele, resulting in red colony formation on medium with limiting adenine concentration. Data from two independent transformations (n= number of transformant colonies) were analysed.

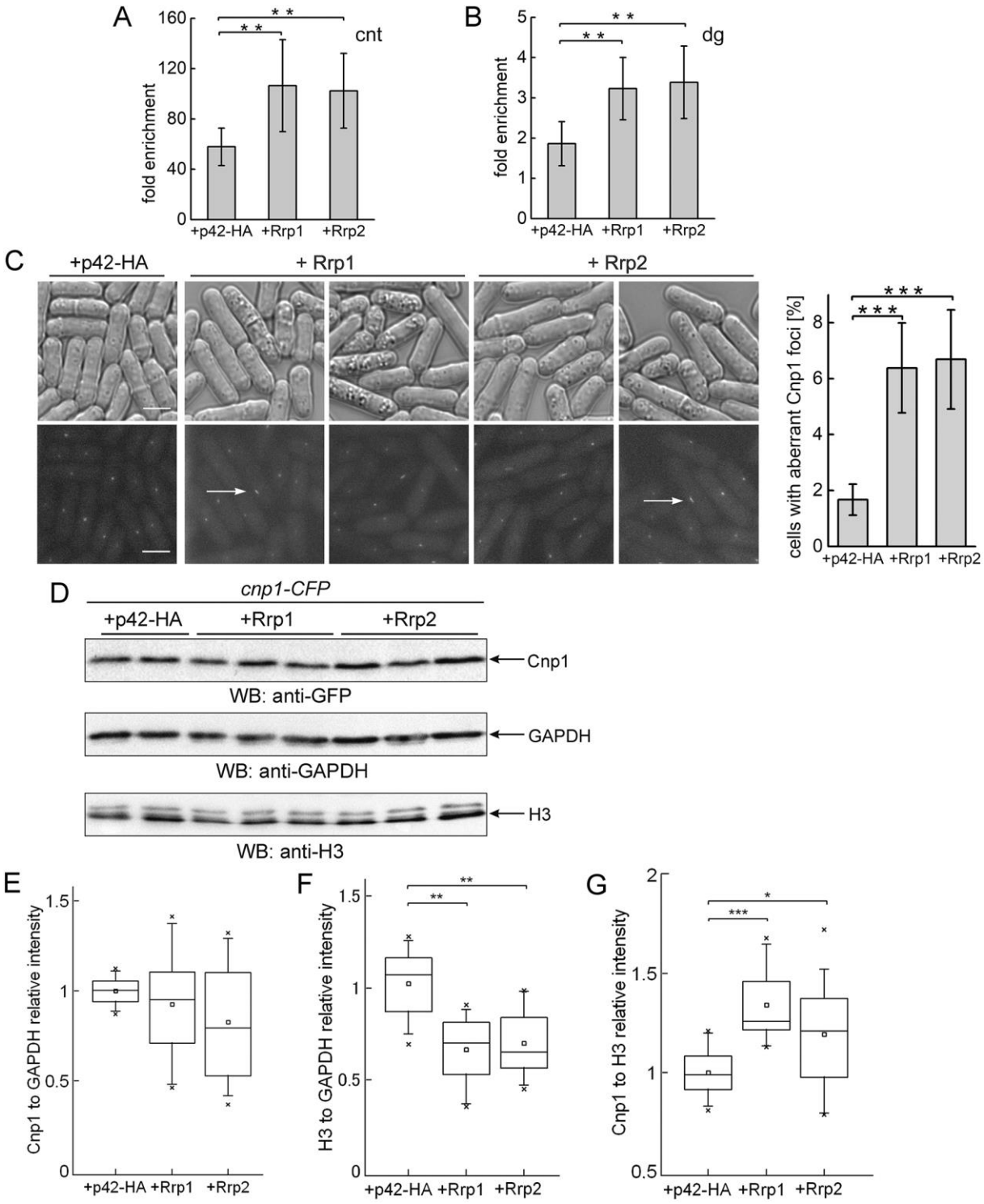

Figure 2 Over-expression of *rrp1+* or *rrp2+* is accompanied by changes in the localisation of centromeric histone H3 variant, Cnp1.

Changes in endogenous Cnp1-CFP localisation at centromere core (A) and outer repeat (B) regions in cells over-expressing *rrp1+* or *rrp2+* as examined by chromatin immunoprecipitation. Fold enrichment is calculated relative to actin control. Primers were

located in centromere core (cnt) and outer repeat (dg) regions. Data were obtained from three independent experiments, for each, real time PCR was repeated at least twice. +p42-HA: empty vector control. (C) *rrp1*+ and *rrp2*+ over-expression leads to the apperance of aberrant Cnp1 foci. *cnp1-CFP* strain transformed with genes for Rrp1-HA or Rrp2-HA as well as empty vector control was examined by fluorescent microscopy. The experiment was repeated four times and the total number of cells counted for each strain was above 2000. Aberrant stretched Cnp1 foci are marked as white arrow. Scale bar represents 5 µm. (D) In cells over-expressing *rrp1*+ or *rrp2*+ the ratio of Cnp1 to H3 increases. Total protein extracts were prepared from *cnp1-CFP* strain over-expressing genes for Rrp1-HA or Rrp2-HA. (D - G) Data were quantified and shown as intensity of Cnp1 signal (E), detected with anti-GFP antibodies, versus anti-GAPDH loading control; relative intensity of anti-H3 signal (F) versus anti-GAPDH loading control and (G) relative intensity of Cnp1 signal, versus anti-H3 signal. All reads were normalised by mean value obtained for vector control samples. Western blots were analysed by ImageLab. A minimum of two independent Western blots from three separate protein isolations from three different transformants were examined.

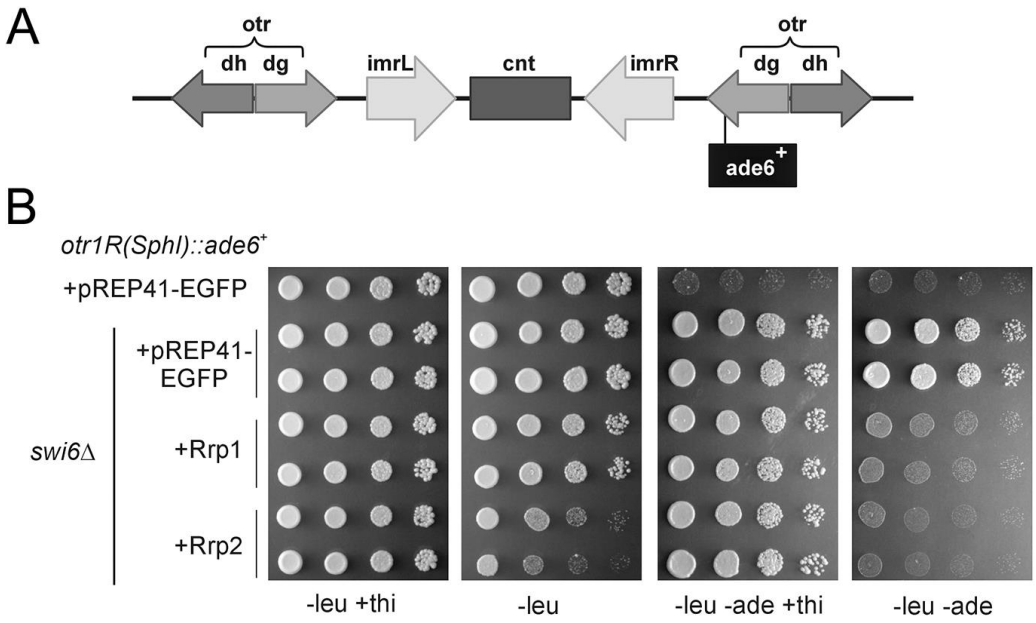

Figure 3 The effect of Rrp1 and Rrp2 on transcriptional silencing at the centromere

(A) The diagram depicting the localisation of the *ade6+* gene in the *dg* region of centromere 1 in a strain (*otr1R(SphI)::ade6+*) used to monitor centromere silencing. (B) Over-expression of *rrp1+* and *rrp2+* reverses the transcriptional de-repression of the *dg-ade6+* gene that is conferred by *swi6*Δ, as determined by the lack of growth on plates devoid of adenine and thiamine (expression inducing conditions).

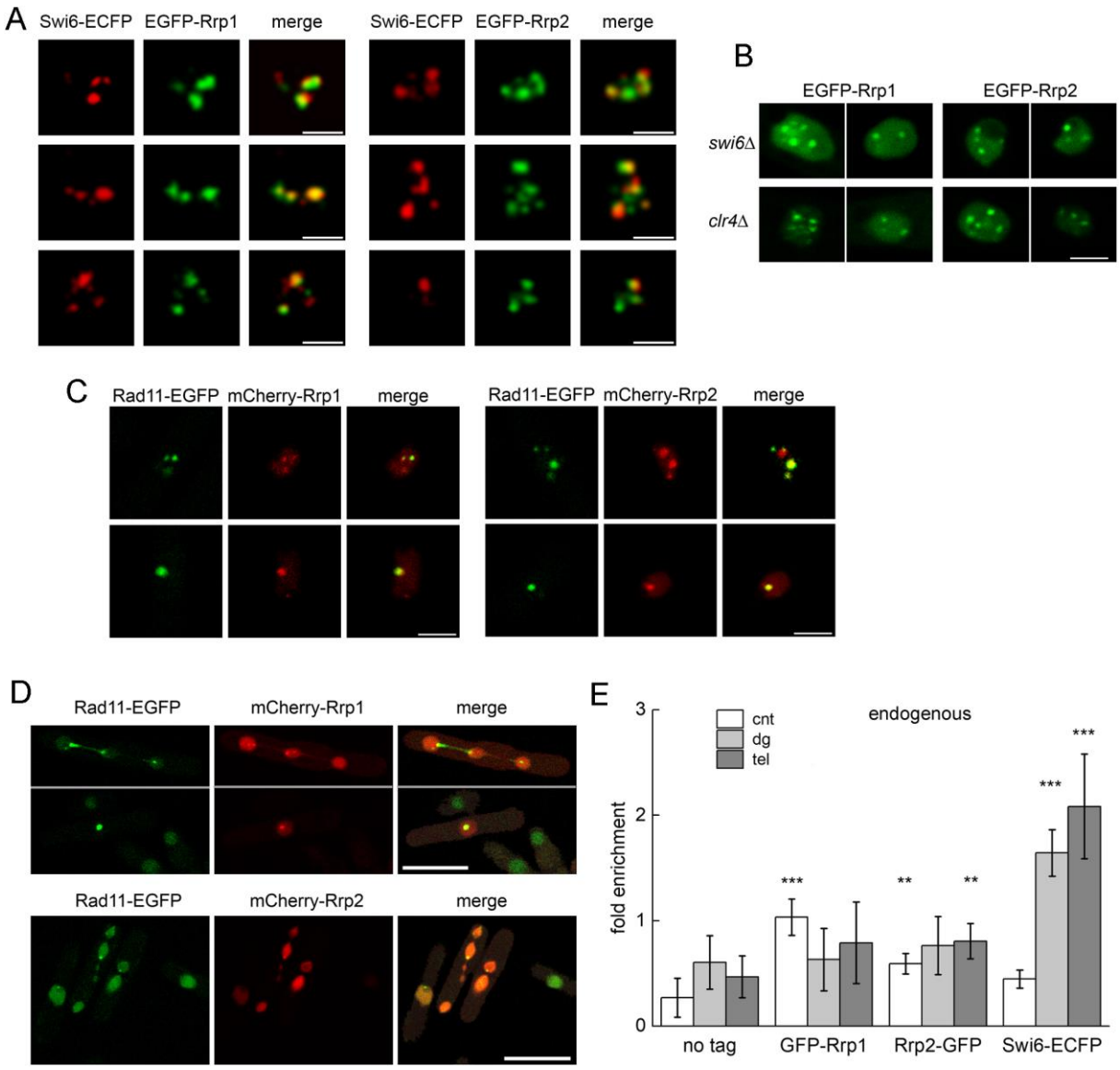

Figure 4 Rrp1 and Rrp2 can bind to centromeric and telomeric DNA

(A) Rrp1 and Rrp2 nuclear foci co-localise in about 40% with foci for Swi6. Strain expressing Swi6-ECFP from endogenous locus was transformed with pREP41 plasmids carrying genes for Rrp1-EGFP or Rrp2-EGFP. Two independent transformants were analysed for each assay and at least 100 cells positive for both ECFP and EGFP signal were counted. Scale bars represent 2 µm. (B) Rrp1 and Rrp2 foci formation is independent from the presence of Swi6 and Clr4. *swi6*Δ and *clr4*Δ strains over-expressing *EGFP-rrp1+*, *EGFP-rrp2+* were examined. Scale bar represents 2 µm. (C) Numerous Rrp1 and Rrp2 nuclear foci co-localise with foci for Rad11. Scale bars represent 2 µm. (D) Rrp1 and Rrp2 are present within Rad11 coated fragmented chromosomes and anaphase bridges. Scale bars represent 10 µm. For C and D strain expressing Rad11-GFP from endogenous locus was transformed with pREP41 plasmids carrying genes for Rrp1-mCherry or Rrp2-mCherry. (E) Endogenous Rrp1 and

Rrp2 can bind to centromere and/or telomere region as shown by chromatin immunoprecipitation. Fold enrichment is calculated relative to actin control. Primers were located in centromere core (cnt), outer repeat (dg) and telomere (tel) regions. Strain expressing endogenous Swi6-ECFP was used as a positive control. Data were obtained from four independent experiments, real time PCR was repeated twice.

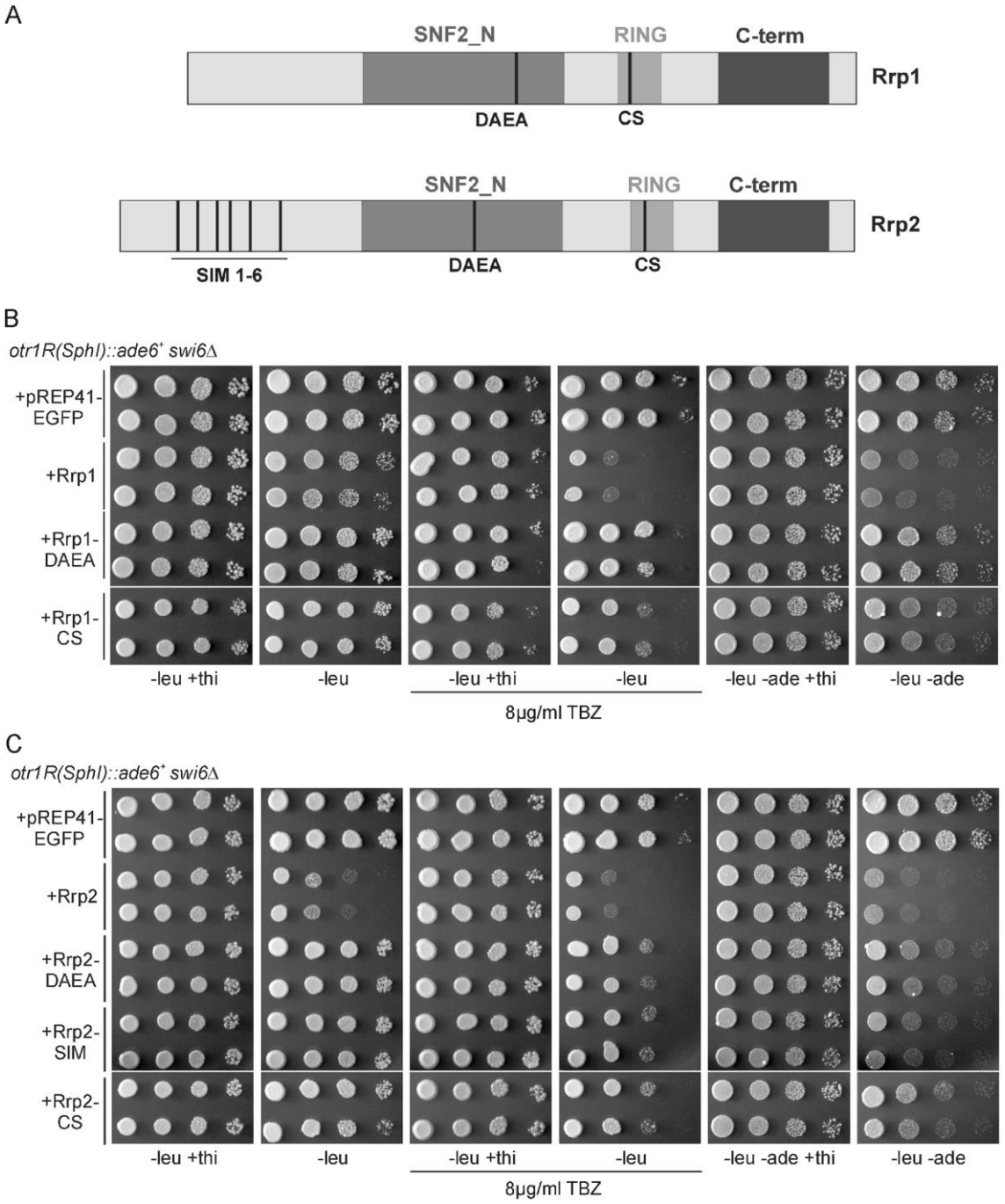

Figure 5 Translocase activity and RING domain of Rrp1 and Rrp2 have distinct roles in the maintenance of centromere

Rrp1 and Rrp2 have a complex domain structure and (A) mutations abolishing their putative SWI2/SNF2 DNA translocase (DAEA) and ubiquitin ligase (CS) activity and SUMO binding (SIM) are shown. Functional Rrp1 translocase and an intact RING domain are required for toxicity, TBZ sensitivity and the silencing of *dg-ade6+* gene (B), whereas for Rrp2 (C) all activities are important for toxicity and TBZ sensitivity but SIM motifs are not required for

silencing of *dg-ade6+* gene. Cells were transformed with plasmids harbouring genes for wild type or mutated versions of respective proteins and the ability of the constructs to support growth on plates with TBZ, as well as to repress growth on plates without adenine under conditions inducing gene expression was assessed. TBZ was added to the plates at the indicated concentrations.

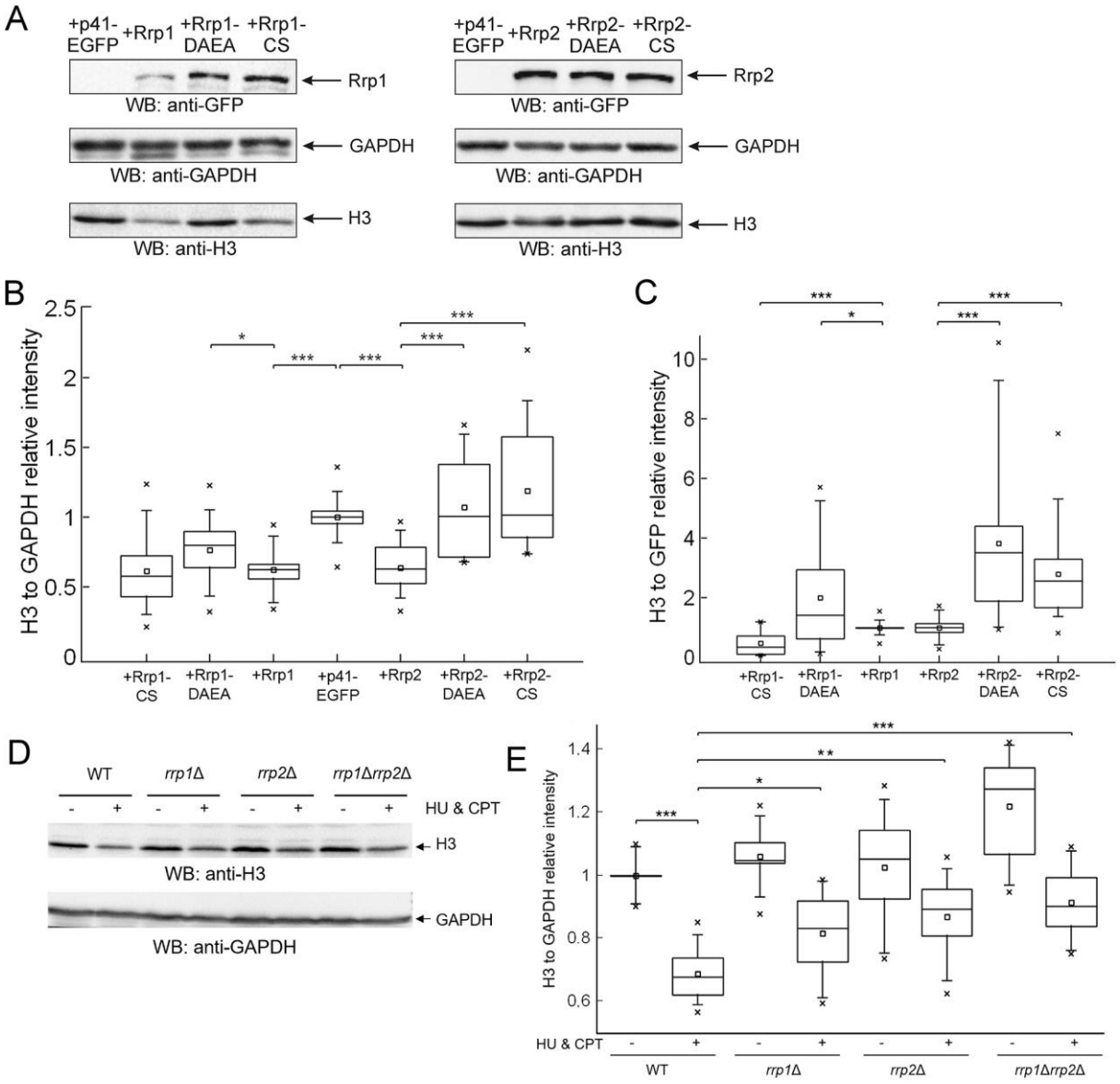

Figure 6 Rrp1 and Rrp2 role in centromere function may involve modulation of histone H3 levels on chromatin

(A) The decrease of histone H3 levels on chromatin seen in cells over-expressing *rrp1*+ or *rrp2*+ differentially depends on their ATPase and RING domains. Total protein extracts were prepared from cells over-expressing genes encoding wild type and mutated forms of Rrp1-GFP or Rrp2-GFP. (B) Data were quantified and are shown as relative intensities of anti-H3, versus anti-GAPDH loading control. Reads were normalised by mean value obtained for vector control samples. (C) Relative intensity of anti-H3 signal, versus Rrp1 or Rrp2 signal, detected with anti-GFP antibodies. Reads were normalised by mean value obtained for *rrp1*+ or *rrp2*+ samples. (D) The decrease of histone H3 levels on chromatin that is induced by DNA damage is partially dependent on the presence of Rrp1 and Rrp2. Total protein extracts

were prepared from studied strains incubated in the presence or absence of HU and CPT. (E) Data were quantified and are shown as relative intensities of anti-H3 signal normalised to anti-GAPDH loading controls. Reads were normalised by mean value obtained for the untreated wild type control sample. Western blots were analysed by ImageLab. A minimum of two independent Western blots from three separate protein isolations from respective strains or three different transformants were examined.

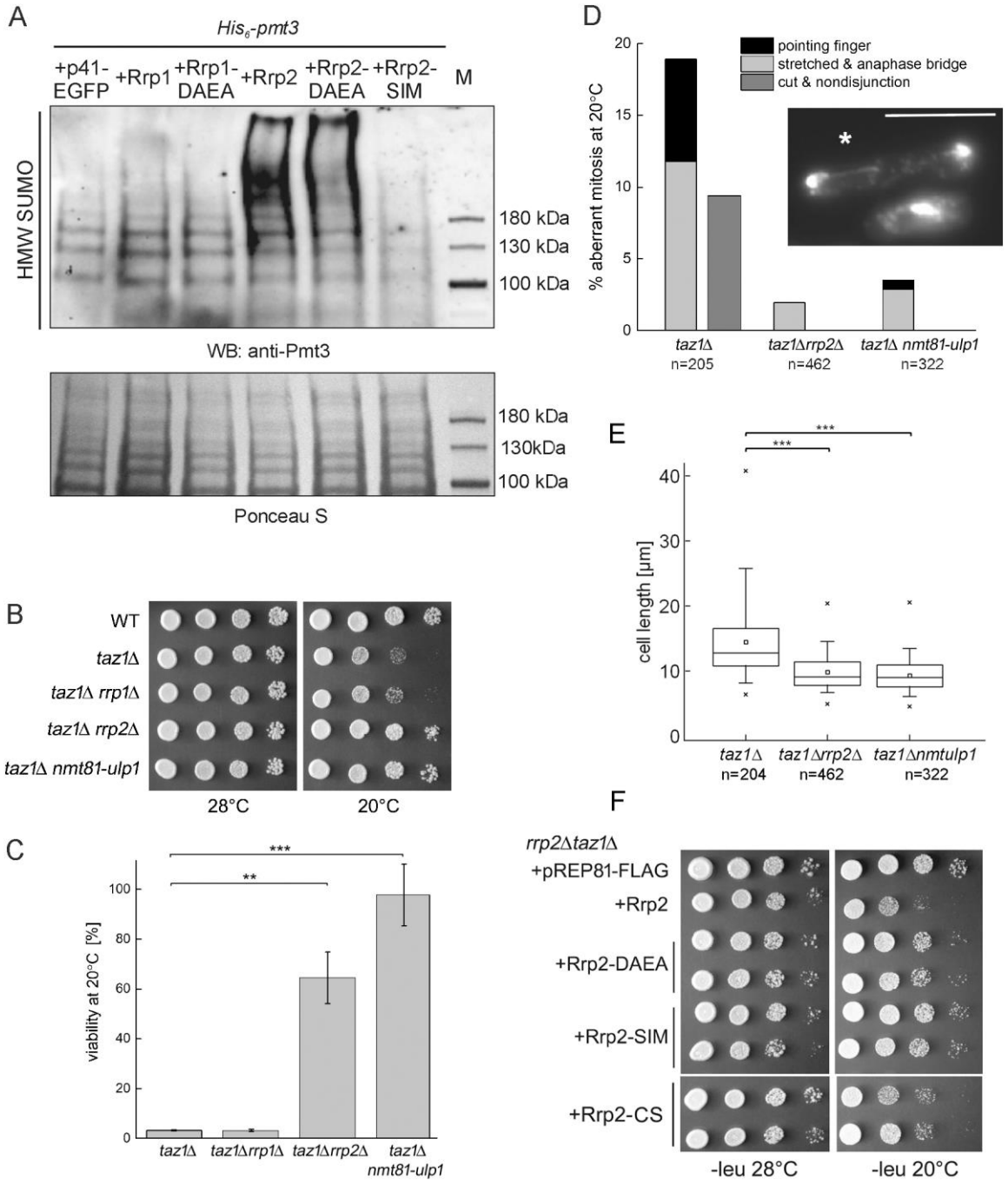

Figure 7 Deletion of *rrp2+* rescues *taz1Δ* telomere entanglement phenotypes

(A) HMW SUMO conjugates accumulate when *rrp2+* but not *rrp1+* is over-expressed and functional Rrp2 SIM motif is essential. The strain with *His$_6$-pmt3* was transformed with empty vector pREP41-EGFP as control and plasmids harbouring genes for wild type or mutated versions of respective proteins. After 24 h growth in minimal medium in absence of thiamine total protein extracts were isolated and subjected to Western blot analysis. SUMOylated proteins were detected with anti-Pmt3 polyclonal serum. Deletion of *rrp2+* rescues *taz1Δ*

mutant's temperature sensitivity seen as (B) growth inhibition when serial dilutions of tested strains were incubated at 20°C, and (C) the differences in viability of cultures grown at 20°C as compared to 28°C. The error bars represent the standard deviation about the mean values, the experiment was repeated at least three times. (D) Decrease of the characteristic *taz1*Δ mutant anaphase defects (telomere specific pointing-finger structure is marked as *) and chromosome breakage and/or missegregation after *rrp2+* deletion. Cultures of respective strains were grown at 20°C for 2 days and their nuclei stained with DAPI. The experiment was repeated twice and the total number of cells counted for each strain (n) is shown below. Scale bar represents 10 µm. (E) Checkpoint activation, observed as cell elongation, is reduced in the double mutant *taz1*Δ*rrp2*Δ. (F) ATPase activity and SUMO binding are responsible for Rrp2 toxicity in *taz1*Δ mutant. *taz1*Δ*rrp2*Δ double mutant was transformed with empty vector pREP81-FLAG, vector carrying wild type and mutated forms of *rrp2+* gene and the ability of the constructs to repress growth at 20°C under expression induction conditions was assessed.

Table S1 Strains used in this study

Strain	Genotype	Reference
YA254 (WT)	ura4-D18, leu1-32, his3-D1, arg3-D1, h90	(Akamatsu et al., 2003)
*rrp1*Δ-1	rrp1D::kanMX6, ura4-D18, leu1-32, his3-D1, arg3-D1, h90	lab stock
*rrp2*Δ-1	rrp2D::kanMX6, ura4-D18, leu1-32, his3-D1, arg3-D1, h90	lab stock
*rrp1*Δ	rrp1D::natMX, his3-D1, leu1-32, ura4-D18, arg3-D1, h90	lab stock
*rrp2*Δ	rrp2D::natMX, his3-D1, leu1-32, ura4-D18, arg3-D1, h90	lab stock
*rrp1Δ rrp2*Δ	rrp1D::kanMX6, rrp2D::natMX, his3-D1, leu1-32, ura4-D18, arg3-D1, h90	lab stock
BX5	His_6-pmt3, ura4-D18, leu1-32, ade6-210, h90	(Xhemalce et al., 2004)
AMC377	rad11-GFP:: kanMX6, ura4-D18, leu1-32, his3-D1, h+	lab stock
GFP-Rrp1	loxP-GFP-Rrp1-loxM, ura4-D18, leu1-32, h+	a
Rrp2-GFP	Rrp2-GFP::loxP kanMX6 loxM, ura4-D18, leu1-32, ade6-704, h+	lab stock
CJ01	ura4-D18, leu1-32, his3-D1, arg3-D1, ade6-m210, Chr16 ade6-m216, h+	b
*clr4*Δ	clr4::LEU2, ura4-D18, ade6-210, h+	c
*clr4*Δ-1	clr4::LEU2, his3-D1, ura4-D18, arg3-D1, leu1-32, h-	a
*clr4*Δ*rrp1*Δ	rrp1:: natMX, clr4::LEU2, his3-D1, ura4-D18, arg3-D1, leu1-32, swi+/-	a
*clr4*Δ*rrp2*Δ	rrp2:: natMX, clr4::LEU2, his3-D1, ura4-D18, arg3-D1, leu1-32, swi+/-	a
YA728	swi6-ECFP, his3-D1, ura4-D18, arg3-D1, leu1-32, Msmt-0	d
FY3138	ade6-DN/N, leu1-32, ura4-D18, otr1R(SphI)::ade6+, h+	(Ekwall et al., 1999)
FY3138 *rrp1*Δ	rrp1D::kanMX6, ade6-DN/N, leu1-32, ura4-D18, otr1R(SphI)::ade6+, h+	a
FY3138 *rrp2*Δ	rrp2D::kanMX6, ade6-DN/N, leu1-32, ura4-D18, otr1R(SphI)::ade6+, h+	a
FY3138 *swi6*Δ	swi6D::natMX, ade6-DN/N, leu1-32, ura4-D18, otr1R(SphI)::ade6+, h+	a
FY3138 *swi6*Δ *rrp1*Δ	swi6D::natMX, rrp1D::kanMX6, ade6-DN/N, leu1-32, ura4-D18, otr1R(SphI)::ade6+, h+	a
FY3138 *swi6*Δ *rrp2*Δ	swi6D::natMX, rrp1D::kanMX6, ade6-DN/N, leu1-32, ura4-D18, otr1R(SphI)::ade6+, h+	a
FY3138 *clr4*Δ	clr4::LEU2, ade6-DN/N, leu1-32, ura4-D18, otr1R(SphI)::ade6+, h+	a
*rad57*Δ	rad57D::his3+, ura4-D18, leu1-32, his3-D1, arg3-D1, Msmt0	(Akamatsu et al., 2003)
*sfr1*Δ	sfr1D::arg3, arg3-D4, ura4-D18, leu1-32, h-	lab stock
*swi5*Δ	swi5D::his3+, ura4-D18, leu1-32, his3-D1, arg3-D1, swi+/-	(Akamatsu et al., 2003)
*rrp1*Δ *rad57*Δ	rrp1D::kanMX6, rad57D::his3+, ura4-D18, leu1-32, his3-D1, arg3-D1, Msmt0	lab stock

rrp2Δ rad57Δ	rrp1D::kanMX6, rad57D::his3+, ura4-D18, leu1-32, his3-D1, arg3-D1, Msmt0	lab stock
FY 4229	CFP-cnp1::kanMX6, ura4-D18, rad22::YFP-kanMX6, sad1::sRed-Leu2+, h?	(Li et al., 2013)
KK821	CFP-cnp1::kanMX6, ade6-704, ura4-D18, leu1-32, h?	a
JCF1779	taz1::ura4+, nmt81-ulp1::kanMX6, ura4-D18, his3-D1, leu1-32, ade6-210, h-	(Rog et al., 2009)
taz1Δ	taz1::ura4+, his3-D1, leu1-32, ura4-D18, arg3-D1, h-	a
taz1Δ rrp1Δ	taz1::ura4+, rrp1::natMX, his3-D1, leu1-32, ura4-D18, arg3-D1, h90	a
taz1Δ rrp2Δ	taz1::ura4+, rrp2::natMX, his3-D1, leu1-32, ura4-D18, arg3-D1, h90	a

a - this work
b - a gift from Jo Murray
c - a gift from Felicity Watts

Table S2 Plasmids used in this study

Plasmid	Reference
pREP41-EGFP	(Craven et al., 1998)
pREP41-EGFP-Rrp1	a
pREP41-EGFP-Rrp1-FLAG	a
pREP41-EGFP-Rrp1-DAEA-FLAG	a
pREP41-EGFP-Rrp1-CS-FLAG	a
pREP41-EGFP-Rrp2	a
pREP41-EGFP-Rrp2-FLAG	a
pREP41-EGFP-Rrp2-DAEA-FLAG	a
pREP41-EGFP-Rrp2-SIM-FLAG	a
pREP41-EGFP-Rrp2-CS-FLAG	a
pREP42-EGFP	b
pREP42-EGFP-Rrp1	b
pREP42-EGFP-Rrp2	b
pREP41-mCherry	b
pREP41-mCherry -Rrp1	b
pREP41-mCherry -Rrp2	b
pREP42-HA	(Craven et al., 1998)
pREP42-HA-Rrp1	b
pREP42-HA-Rrp2	b
pREP81-FLAG	b
pREP81-Rrp1-FLAG	a
pREP81-Rrp2-FLAG	a
pDUAL-Prrp2-GFP-Rrp2-SIM(1-6)*	(Wei et al., 2017)

a - this study
b - laboratory stock

Table S3 Primers used in this study:

Cloned gene	Primer name	Primer sequence
FLAG	REP3flag_a_r	ctttatcatcgtcgtccttgtagtcggatcctctagagtcgacatatgatttaac
	REP3flag_b_f	tacaaggacgacgatgataaagactacaaggacgacgatgataaagacta
	REP3flag_c_r	gggtcatttatcatcgtcgtccttgtagtctttatcatcgtcgtccttgtagt
	REP3flag_d_f	caaggacgacgatgataaatgacccgggtaaaaggaatgtctcccttgccagtac
Rrp1-FLAG	Rrp1_fwd	caactaattattcgaaacggaattcgaaacgATGGATTCATTGTCTGCATATC
	Rrp1_rev	tttaaatggccggccggtaccTCATGAATTAAGCCCAAATAG
Rrp1-DAEA-FLAG (D397A; E398A)	Rrp1_fwd	caactaattattcgaaacggaattcgaaacgATGGATTCATTGTCTGCATATC
	Rrp1D397A_rev	tatgtgcggcCGCTAGAACAATGCGATAC
	Rrp1E398A_fwd	tgttctagcgGCCGCACATACCATTCGT
	Rrp1E398A_rev	tttaaatggccggccggtaccTCATGAATTAAGCCCAAATAGATATAG
Rrp1-CS-FLAG (C609S)	R1c609sN_fwd	tttctgacttatagtcgctttgttaaatcatATGGATTCATTGTCTGCATATC
	R1c609sN_rev	caaacaaggatctagACTAACACTACAGTTGAAATCC
	R1c609sC_fwd	aactgtagtgttagtCTAGATCCTTGTTTGGCTC
	R1c609sC_rev	tagtctttatcatcgtcgtccttgtagtcggatccTGAATTAAGCCCAAATAGATATAG
Rrp2-FLAG	Rrp2_fwd	caactaattattcgaaacggaattcgaaacgATGAGAAATAATACAGCTTTTGAAC
	Rrp2_rev	tttaaatggccggccggtaccTTATCGTGATGACATTCCAAATAAAAATG
Rrp2-DAEA-FLAG (D539A; E540A)	Rrp2D539A_fwd	caactaattattcgaaacggaattcgaaacgATGAGAAATAATACAGCTTTTGAAC
	Rrp2D539A_rev	tttgagcggcCGCCAATATAACTCGATACC
	Rrp2E540A_fwd	tatattggcgGCCGCTCAAACTATCAAAAAC
	Rrp2E540A_rev	tttaaatggccggccggtaccTTATCGTGATGACATTCCAAATAAAAATG
Rrp2-CS-FLAG (C749S)	R2Nc749s_fwd	tttctgacttatagtcgctttgttaaatcatATGAGAAATAATACAGCTTTTGAAC
	R2Nc749s_rev	tgcaacaacatccatGGATAAGGAGCATTGCAAC
	R2Cc749s_fwd	caatgctccttatccATGGATGTTGTTGCAGAAC
	R2Cc749s_rev	tagtctttatcatcgtcgtccttgtagtcggatccTCGTGATGACATTCCAAATAAAAATG
Primers used for qPCR in ChIP experiments		
act1	act_F	cgccgaacgtgaaattgttcgtga
	act_R	aagggaggaagattgagcagcagt
centromere *cnt*	cnt_F	caaccgttgcaacttacatcagca
	cnt_R	ccggtcgccaaatagcaatgagat
centromere *dg*	dg_F	taccgtgattagccttactccgca
	dg_R	accgcaagatagagtaggatgggt
telomere	tel_F	tcaaagttggcgacgttgctgatg
	tel_R	aagcaatgtgtggagcaacagtgg

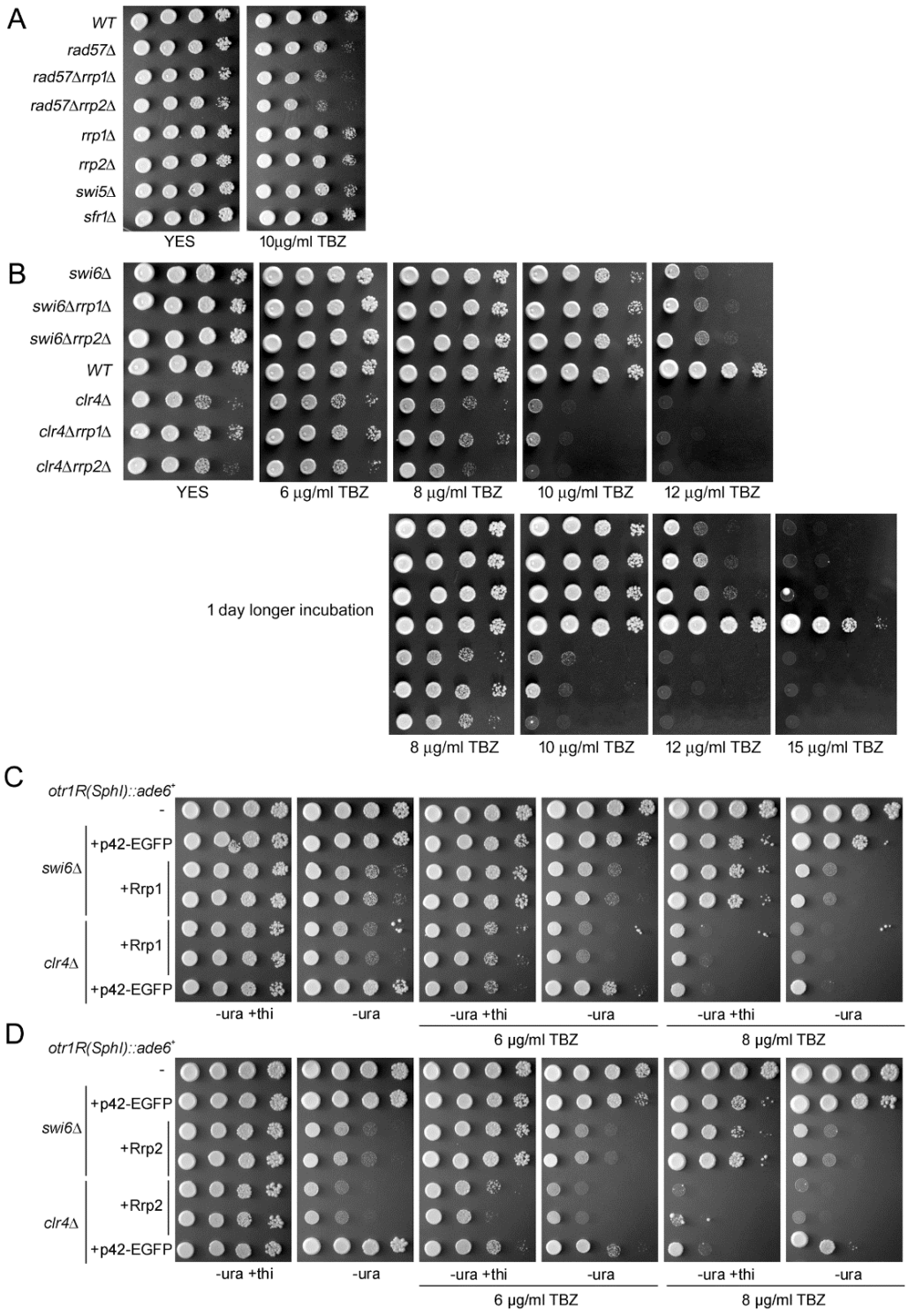

Fig. S1 Rrp1 and Rrp2 may be implicated in centromere function

(A) Strains devoid of genes for Swi5-Sfr1 mediator complex and Rrp1 or Rrp2 are not sensitive to TBZ. *rad57*Δ is sensitive and deletion of *rrp1*+ or *rrp2*+ in this mutant increases this sensitivity. (B) Deletion of *rrp1*+ or *rrp2*+ decreases TBZ sensitivity in *swi6*Δ mutant while in *clr4*Δ mutant, deletion of *rrp1*+ but not *rrp2*+ rescues its growth defect. Rrp1 and Rrp2 act independently of Swi6 and Clr4 as over-expression of (C) *rrp1*+ and (D) *rrp2*+ sensitizes *swi6*Δ and *clr4*Δ cells to TBZ. TBZ was added to the plates at indicated concentrations.

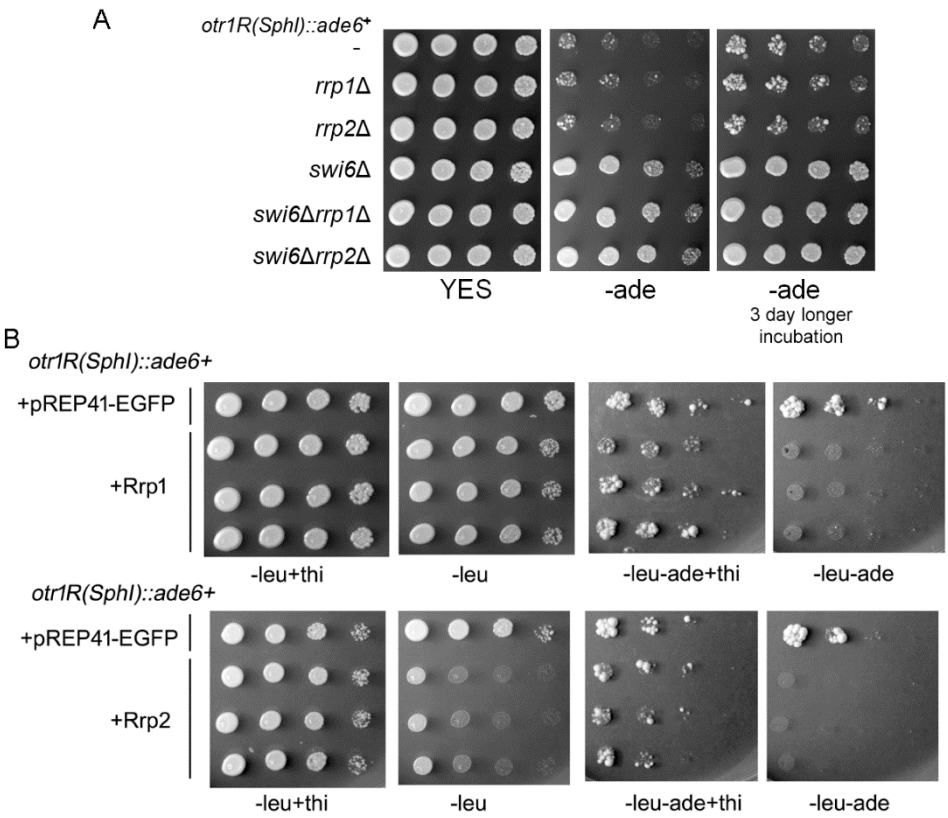

Figure S2 The effect of Rrp1 and Rrp2 on transcriptional silencing at the centromere

(A) Deletion of *rrp1+* or *rrp2+* has no effect on the silencing of *dg-ade6+* gene in *swi6+* or *swi6*Δ backgrounds, monitored by the ability of these mutants to grow on plates without adenine. (B) *rrp1+* or *rrp2+* over-expression results in an increase in repression of the *dg-ade6+* gene in *swi6+* background as determined by the lack of growth on plates devoid of adenine and thiamine (expression inducing conditions).

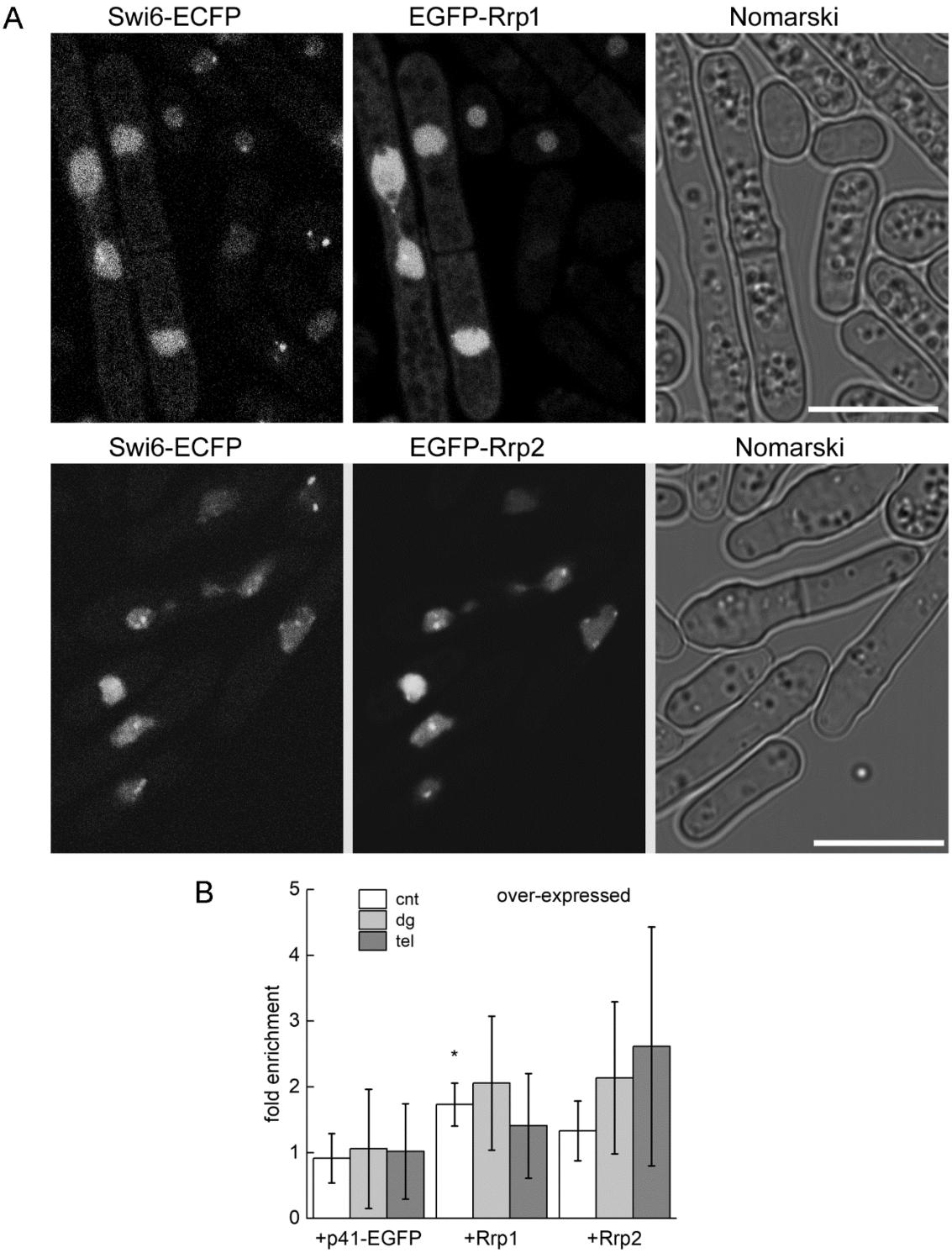

Fig. S3 Over-expressed Rrp1 and Rrp2 can bind to centromere and/or telomere region.

(A) Rrp1 and Rrp2 are present within Swi6–coated fragmented chromosomes. Strain expressing Swi6-ECFP from endogenous locus was transformed with pREP41 plasmids carrying genes for Rrp1-EGFP or Rrp2-EGFP. Scale bars represent 10 μm. (B) Centromere and/or telomere binding of overproduced Rrp1-EGFP or Rrp2-EGFP was examined by chromatin immunoprecipitation. Fold enrichment is calculated relative to actin control. Primers were located in centromere core (cnt), outer repeat (dg) and telomere (tel) regions. Data were obtained from two independent experiments, real time PCR was repeated twice.

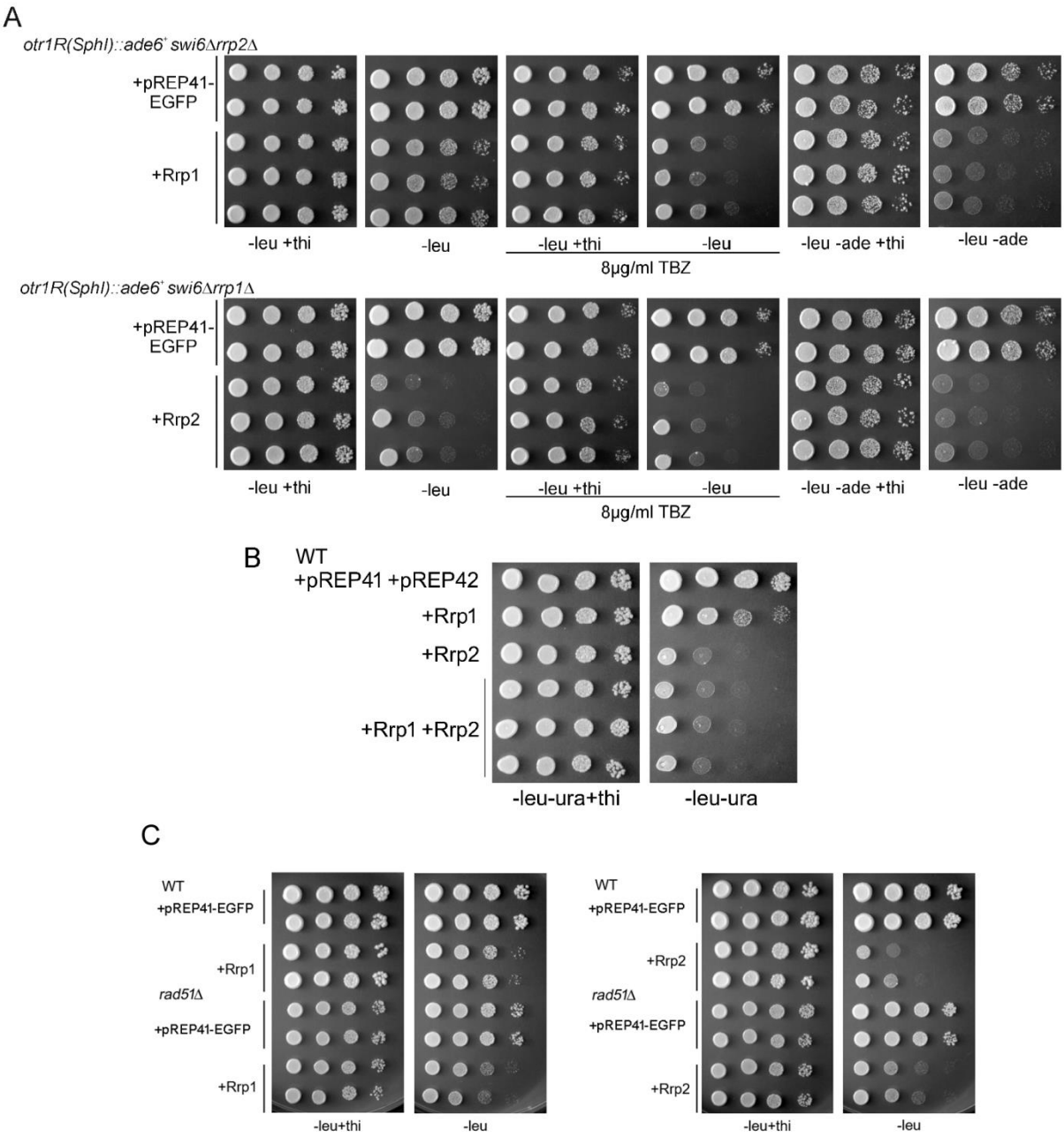

Fig. S4 Interdependence of *rrp1+* and *rrp2+* over-expression phenotypes

(A) Centromere functions of Rrp1 and Rrp2 are not dependent on the presence of the other respective paralogue. Reporter *swi6Δdg-ade6+* strain with *rrp1+* or *rrp2+* deletion was transformed with pREP41-EGFP-Rrp2 or pREP41-EGFP-Rrp1 plasmid, respectively. Loss of viability and increased TBZ sensitivity are observed as growth inhibition while transcriptional repression by the ability to grow on plates lacking adenine under expression induction conditions (plates lacking thiamine). (B) Growth defect resulting from simultaneous over-expression of both genes is similar to the effect caused by *rrp2+* over-expression. Strains were transformed with empty pREP41-EGFP or pREP42-EGFP vector (carrying respectively leucine or uracil marker gene) as control and corresponding plasmids with *rrp1+* and *rrp2+* genes. Loss of viability is observed as growth inhibition on plates lacking thiamine (expression induction conditions). (C) Only growth defect resulting from *rrp2+* over-expression is dependent on the presence of Rad51 recombinase.

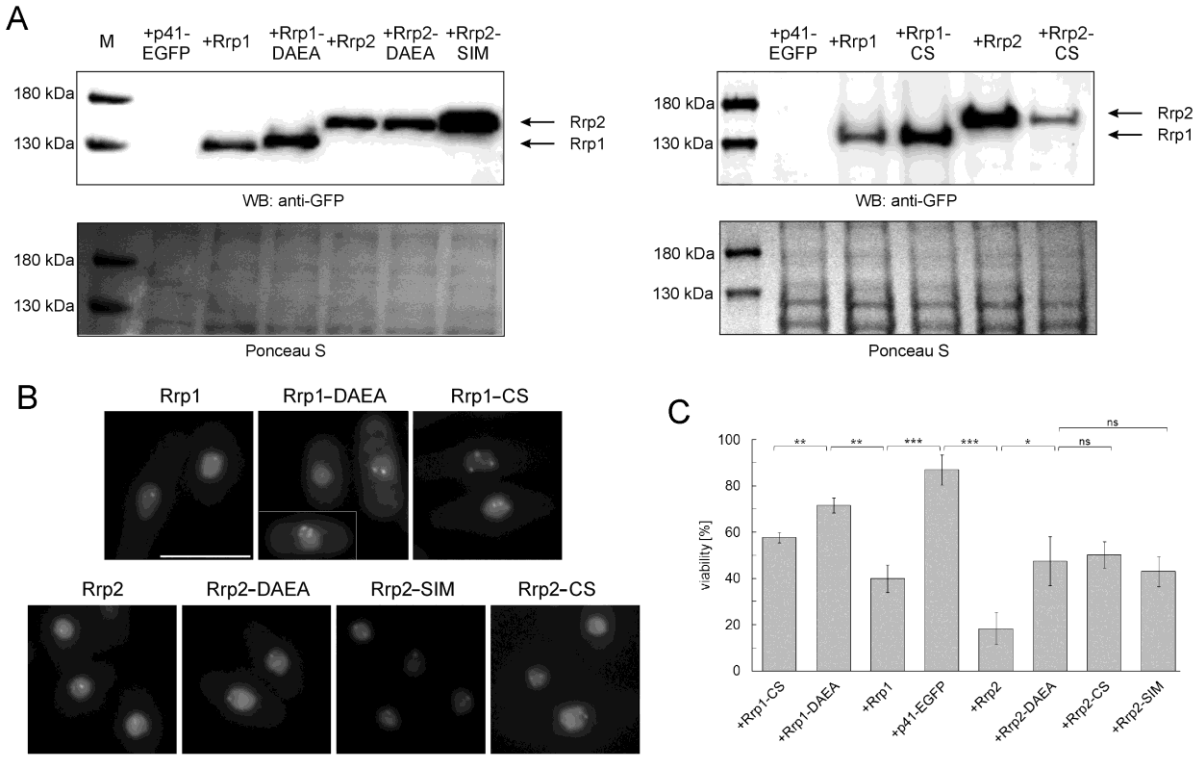

Fig. S5 Analysis of the functionality of mutated versions of Rrp1 and Rrp2 proteins

WT strain over-expressing wild type or mutated versions of *rrp1*+ or *rrp2*+ from pREP41-EGFP plasmid was used. (A) All proteins are expressed as confirmed by Western blot with anti-GFP antibodies of proteins isolated from cultures incubated for 24 h without thiamine (expression inducing conditions). (B) All proteins form foci in the nucleus. (C) All domains contribute to the loss of viability conferred by *rrp1*+ or *rrp2*+ over-expression. Loss of viability was determined for strains growing in the presence and absence of thiamine, as compared to empty vector pREP41-EGFP control. The experiment was repeated at least twice for two independent transformants. The error bars represent the standard deviation about the mean values. Student's t-test was used to calculate the P-value (* $0.01 < \text{P-value} \leq 0.05$, ** $0.001 < \text{P-value} \leq 0.01$, *** $\text{P-value} \leq 0.001$). Cells from cultures used in (A) were analysed by fluorescence microscopy (B). Scale bar indicates 10 µm.

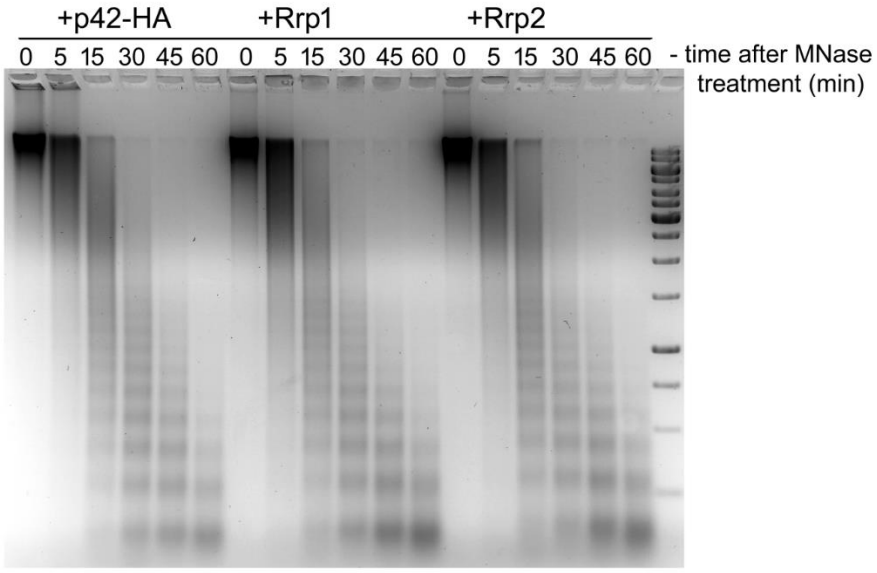

Fig. S6 Global nucleosome spacing is not altered by Rrp1 or Rrp2 overproduction.

MNase assay of chromatin extracts from cells transformed with plasmids carrying genes for Rrp1-HA or Rrp2-HA and. Simply safe stained gel with partially digested chromatin samples treated for different times with 5 U/ml MNase. The assay was repeated twice.